CERN/SPSC/77-7
SPSC/P 80/Add.1
25.01.1977

PROPOSAL TO STUDY NEGATIVELY CHARGED HYPERON INDUCED REACTIONS AND $\bar{p}$ ANNIHILATIONS AT SPS ENERGIES†

Bari[1]††, Rutgers[2], Strasbourg[3]

H. Braun[3], F. Brochard[3]*, E.B. Brucker[2], T. Chiaradia[1], F. Etienne[3], C. Favuzzi[1], A. Fridman[3], J-P. Gerber[3], G. Germinario[1], P. Gorodetzky[3]*, L. Guerriero[1], E. Jegham[3], H. Johnstad[3], P. Juillot[3], J-R. Lutz[3], C. de Marzo[1], G. Maurer[3], R. Meunier**, A. Michalon[3], R. Plano[2], F. Posa[1], H. Sanders[2], G. Selvaggi[1], C. Voltolini[3], F. Waldner[1], T. Watts[2], R. Windmolders***

The aim of this experiment is to study Σ^- and $\bar{\Xi}$ induced reactions at 250-350 GeV/c as well as $\bar{p}N$ annihilations in the 100-250 GeV/c momentum range. The experimental set up includes a streamer chamber coupled to a spot focusing Cerenkov counter (S.C.S.F.) for the identification of fast outgoing particles. With the 400 GeV/c extracted proton beam it is possible to design and build a high intensity hyperon beam with a wide momentum range. Coupled to the S.C.S.F. this will become a new and unique CERN facility for the North Area.

The momenta of high energy tracks will be measured with an accuracy of at least 3% by means of a downstream spectrometer made of multiwire proportional chambers and bending magnets. This instrument presents the important feature of being self triggered on the interaction taking place in the target. The signature is one leading particle (Y^- or $\bar{p}$) identified in mass, momentum and emission angle. Other counters and hodoscopes can add more conditions to the trigger. The beam particle for the interaction is identified by a multiplexed DISC.

Since there are yet no data on hyperon collisions at very high energy, the proposed experiment will provide new information in many physical topics. As a first step we plan to study multiplicity distributions and semi-inclusive reactions such as $YN \to \Sigma^{\pm}X$, ΛX, Ξ^-X, ΩX (Y stands for Σ^- and $\bar{\Xi}^-$). Diffraction dissociation properties of the hyperon will be investigated and a systematic search for new baryonic resonances will be carried out.

The $\bar{p}$ beam will allow us to test and to set up the apparatus. In addition we intend to study multiplicity distributions and $\bar{p}N$ annihilations. The produced π^o's will be detected by lead oxide plates put in the streamer chamber.

The proposed experimental set up will also allow to study the dependence of the production processes and the multiplicity distributions as a function of the atomic weight of the target.

† The experimental part has been studied and worked out in collaboration with R. Meunier from CEN Saclay and F. Rohrbach from CERN (EF Division).

†† To be submitted to INFN

* From the Nuclear Spectroscopy Group, CRN, Strasbourg

** CEN Saclay, Visitor at CERN

***From the University of Mons, Belgium

SUMMARY

1. INTRODUCTION 1

2. PHYSICS PROGRAM 4

3. GENERAL DESCRIPTION OF THE SET UP ... 10

4. THE HYPERON BEAM 14

5. THE STREAMER CHAMBER AND VERTEX MAGNET 17

6. SPOT FOCUSING DETECTOR 22

7. TRIGGERING AND NUMBER OF EVENTS 30

8. CONCLUSIONS 34

1. INTRODUCTION

1.1. General motivations

During these last years an impressive effort has been devoted to the study of hadron - hadron interactions in the few hundred GeV/c incident momentum region. In this region there is very little information about reactions with incident $\bar{p}$ (1) and practically no information about hyperon induced interactions although there is now an increasing interest in this field (2,3). We are therefore proposing to study reactions using a negatively charged beam of baryonic number $|B| = 1$ at the SPS energies. We intend thus to study $\bar{p}$, Σ^- and Ξ^- collisions with nucleons and also with different kind of nuclei.

One has to emphasize that the proposed experiment is complementary to the E H S project. Indeed we want to investigate processes which cannot be studied with a bubble chamber as the number of wanted particles (i.e. the hyperons) represents only a small fraction of the beam (of the order of 1 %). Therefore we intend to use a spectrometer containing a streamer chamber which can be triggered on a given beam particle and on an interaction in the target, both of them obtained with high performances Cerenkov counters (multiplexed Disc and Spot focusing).

Because of the lack of high energy data on hyperon interactions the exact incident momenta that should be used for this experiment are not really crucial. Nevertheless we are proposing to use hyperon incident momenta of 250 to 350 GeV/c. In the following we will only discuss the first step of our hyperon study, i.e. the point at 250 GeV/c.

As a first approach into the new field of hyperon physics we would like to collect as much general information as possible. By this we mean that we want to obtain first of all information about multiplicity distributions and also about the semi-inclusive reactions $YN \to \Sigma^{\pm} n_c$, Λn_c, $\Xi^- n_c$, $\Omega^- n_c$. Here Y denotes a Σ^- or Ξ^- particle and n_c is the associated number of charged particles. The knowledge of the YN multiplicity distribution and their associated statistical moments will allow us to make a comparison with other type of hadron-hadron collisions. In particular we will stress out the influence of the

strangeness in the quantities just mentioned as we will have initial states having S = -1 and -2. This study will be completed by investigating the multiplicity distributions of systems recoiling against the leading particle or against any charged particle emitted with the Feynman variable $x \sim 0.9$. We will thus be able to select recoiling system with given quantum number and still to see their influence on the multiplicity distribution (see sect.2).

Additional motivations of the present proposal consists in the possibilities to study the single and double diffraction dissociation processes and to search for new strange baryonic resonances. As there is a strange baryon in the initial state, we expect to observe copious strange resonance production (i.e. Y^*, Ξ^* and Ω^*). A study of the production of these resonances is envisaged. In particular we intend to see how the resonance production is correlated with the number of charged outgoing particles.

There is no reliable estimate of the Ω^- flux, however the Disc in the beam will continuously tag these particle and Ω^- triggers will always be operative.

The second aspect of our experiment consists to study $\bar{p}$ annihilations. Apart of the physical motivations which will be explained below, the fact that we will have to our disposal a $\bar{p}$ beam will allow us to test and to set up our apparatus. Then we will be able to achieve our main goal which is the study of hyperon induced reactions.

For the $\bar{p}$ part of our experiment we would like to study primarily the annihilation reactions as function of the incident momentum in the range of 100 – 250 GeV/c. In particular we intend to obtain information about multiplicity distributions and statistical moments for the annihilation reactions as well as for the non-annihilation ones. We also plan to investigate the correlation between the average number of produced π^o with the associated number of charged outgoing particles.

1.2 - Choice of apparatus

The general features of our physics program presented briefly above define almost completely the instrument to be used for the proposed experiment. We need a device allowing the detection of charged particles with a minimum of biases. Furthermore, the momentum of the fast tracks have to

be measured with a sufficient accuracy to search for Y^*, Ξ^* and Ω^* resonances. Our instrument must also be able to identify particles or at least the hyperons which are emitted in the forward direction.

These considerations and the necessity to work with an unseparated beam lead us to use a streamer chamber coupled to a spot focusing Cerenkov counter (S.C.S.F.) and a downstream spectrometer. The streamer chamber which will in fact be used as a vertex detector is envisaged to operate in a magnetic field. We will thus be able to measure the small momentum tracks and to observe a non negligible fraction of the Λ hyperons decays. The conjunction of the streamer chamber and the downstream spectrometer as shown schematically in fig.1.1, will permit the measurement of fast outgoing tracks. For identifying the particles emitted in the forward direction, we intend to use the spot focusing device now developed at CERN. As described below (sect.6), this apparatus will be able to identify and measure the emission angle of all the charged particles entering simultaneously in it.

The instrument we want to build is complex but very powerful and flexible. As will be seen below, we will be able to study the annihilation reactions and to obtain representative samples of semi-inclusive reactions containing identified $\Sigma^{\pm}$, Λ, Ξ^- or Ω^- particles in the final state. Most of these particles are expected to present a strong leading particle effect and will then be detected with a great efficiency by our detector (sse sect. 3). Our instrument combines the advantage related to an optical vertex detector with those obtained in usual counter experiments. In other words we will have at our disposal an almost 4π vertex detector in which pattern recognition problems are minimized and which will allow us to explore phenomena with a cross section as low as a few tens of μb.

In sect. 2, we will discuss in some more detail our physics program. Then we will present the general features of our equipment (sect. 3) and subsequently a more detailed description of its various components (sect. 4 through 6). Sect. 7 will be devoted to the discussion of the various triggers needed to accomplish our physics program.

2. PHYSICS PROGRAM

As already stated above the aim of this experiment is twofold in the sense we want to study hyperons and $\bar{p}$ induced reactions. In both cases we would like to have an access to different initial isospin state. Therefore we will use an hydrogen and a deuterium target. In a further stage we will also study the multiplicity distributions and their associated statistical moments as a function of the atomic weight of the target.

For the study of the collision on proton or neutron we plan to use thin high pressure gaseous targets. This will allow us to observe in the streamer chamber most of the tracks having low momenta. For example with a 100 atmospheres H_2 target of 2mm diameter one will see about 115 MeV/c outgoing particles. Thus, in the case of a deuteron target we will be able to observe an important fraction of the spectator protons. In the following we will describe in more detail some typical aspects of our experimental program.

2.1. Hyperons interactions

2.2.1 - Semi-inclusive reactions

As practically nothing is known on hyperon interactions at $\sim$ 250 GeV/c, we will first investigate the semi-inclusive reactions

$$YN \to \Sigma^{\pm} n_c,\ \Lambda n_c,\ \Xi^{-} n_c,\ \Omega n_c\ .$$

The cross sections, the rapidity structure of the charged emitted particles as well as the single particle distributions of the (identified) particle will be measured and compared with other type of hadron-hadron interactions. Factorization properties will be investigated, in particular as a function of different kinematical variables.

By selecting one or even a given number of identified forward particles, we will have reactions having definite quantum numbers exchanged in the t-channel. The influence of these quantum numbers on the single particle distribution will be investigated. The fact that we will have an hyperon beam (S = -1, -2) offers us the possibility to exchange a great variety of quantum numbers.

Furthermore, the study of the reactions $YN \to Yn_c$ will allow us to check the SU(3) nature of the Pomeron. Indeed by taking event where Y is the only charged particle emitted in the $x \sim 1$ region, one expects that

Pomeron exchange will dominate the production process. Then, the single particle distribution associated to the leading particle should be identical to those observed in the same condition in pp interactions if the Pomeron is a pure SU(3) singlet. In any case detailed comparisons between pp and Yp spectra will be made and this for different charged multiplicities.

2.1.2 - Topological cross section and multiplicities

Various works made in the past have shown that the study of charged multiplicities and their associated statistical moments provide some knowledge about the multiparticle production process. The results which will be obtained at 250 GeV/c will allow us to see the influence of the s-channel quantum numbers (and particularly the strangeness) on the multiplicity distributions. Based on the present available high-energy data it appears that multiplicity distributions do not depend strongly from the type of the colliding particles, apart from the exception of $\bar{p}p$ reactions (4)

Nevertheless, differences exist as for instance in the KNO distributions and the behaviour of statistical moments. Even s-channel isospin appears to have an influence on the statistical moments as shown at least by the comparison of $\bar{p}p$ and $\bar{p}n$ data below 100 GeV/c (7) (fig.2.1,2.2). As yet all the comparisons have only be made between colliding particles having a total baryonic number B = 0, 1, 2 and strangeness S = 0, ±1. Therefore, the comparison of our experiment with FNAL results at 150 GeV/c will show the importance of strangeness on the multiplicity distributions and may bring some new insight about multiparticle production processes.

As a complement to the above study, we intend also to investigate the multiplicity distributions associated to the system recoiling against the leading particle or against any particle emitted near $x \sim 1$. This will allow us to isolate systems of definite quantum numbers and to see still their influence on the multiplicity distributions.

Similar studies made with pp (102, 205 and 405 GeV/c) and π^-p (205 GeV/c) [5] have shown that the baryonic number associated to the recoiling system does not appear to have a great influence on the quantities just mentioned.

In any case, by using hyperon beams one will obtain recoiling systems in a great variety of quantum numbers(fig.2.3) allowing us to carry out a systematic study of their influence on the multiplicity distributions. In other words, by selecting forward emitted particles, we will study the cluster of particles associated to the nucleon vertex as a function of the cluster quantum numbers and as a function of its mass M_x (the range of M_x extends from ~2 to ~10 GeV/c^2).

2.1.3. - Diffraction dissociation

We also are interested to study the single and double diffraction dissociation of the incoming particles. Similarly, to the diffraction dissociation of $p \to N^*$ seen in hadron-proton interactions we expect to observe copious $\Sigma^- \to Y^{*-}$ and $\Xi^- \to \Xi^{*-}$ processes. In fact, the diffraction dissociation mechanism will certainly be important because the inital YN system is exotic (in the sense that B = 2). Then, the contribution of the leading exchange degenerate Regge trajectories are expected to cancel, the interactions being then dominated by Pomeron exchange.

We intend in particular to study the following processes:

$$\Sigma^- \to Y^{*-} \quad \hookrightarrow \Lambda\pi^-,\ \Sigma^-\pi^+\pi^- \qquad\qquad \Sigma^- \to Y^{*o}\ \pi^- \quad \hookrightarrow \Sigma^{\pm}\pi^{\mp}$$

$$\Xi^- \to \Xi^{*-} \quad \hookrightarrow \Lambda K^- \qquad\qquad \Xi^- \to \Xi^{*o}\ \pi^- \quad \hookrightarrow \Xi^-\pi^+$$

In fact, it has been predicted by Lipkin [9] that there should be Y^* resonances not discovered yet and which are primarily produced in diffraction dissociation processes. A systematic search for these resonances will be made.

Furthermore, polarization measurement of the Λ whenever they are present among the decay products will help us to determine the spin and parity of these resonances. These new resonances are predicted to be narrow (6) (narrower than the N^*) and will in any case be detected by our apparatus (see Section 3).

In the case that the incident hyperon dissociates into one resonance, we will be able to check whether or not the Gribov-Morrison rule can be applied to strange baryons. To do this, one has to be sure that no other neutral particle will be emitted at the hyperon vertex. Fitting of events will thus be very helpful. At the present stage it is not clear that the beam momentum will be known with a sufficient accuracy to allow four constraints fits. In any case if fits will be possible one will have another way to test the SU(3) nature of the Pomeron. Indeed the diffraction dissociation of the Σ^- for instance into a Y^* belonging to a SU(3) decuplet is not allowed if the Pomeron is a SU(3) singlet. Thus, the identification of the dissociated Y^* or Ξ^* state will bring some additional information about the nature of the Pomeron.

By studying the azimuthal distributions of the outgoing particles [7] one will be able to see whether or not the diffraction interaction data are compatible with helicity conservation in the s or t channel. The measurement of the Λ polarization, whenever they are present in the final state may allow to give some more definite answer. In any case Λ polarization measurements will give further information about diffraction dissociation mechanisms in ΣN as well as in ΞN and ΩN interactions. Finally, we will also study the double diffraction dissociation process for which one expect a cross section of about 0.3 mb (8).

2.1.4. Resonance production

In addition to the investigation concerning the production of resonances in diffraction dissociation we will carry out a systematic search for strange baryonic resonances. These resonances (Y^*, Ξ^*), will certainly be produced abundantly as in many case their productions do not require strangeness exchange.

The proposed experiment is also particularly suitable for searching exotic resonances as $\Sigma^-\pi^-$ and Λp for which some evidences have been reported some years ago [9]. Finally, we will also study the production of non strange resonances and their correlation with the strange ones.

2.1.5. - Strange particle production

One of the striking results obtained in the recent experiment made at FNAL with the 30" hybrid system consists in the rapid rise of the strange particle production. It is not clear yet if these strange particles are produced centrally or are a consequence of the dissociation of the colliding particles. Our apparatus will yield new information about this matter as we may identify the hyperons through their decay in the streamer chamber and the spot focusing system. If one assumes that strange pairs of particles are produced in YN collisions as copiously as in pp ones (fig. 2.4) we will have numerous reactions having three or more strange particles in the final state. We will thus be able to study the strangeness repartition in the c.m. system (local or non local strangeness conservation). A comparison with the charge fluctuations may lead to a better understanding of multiparticle production.

2.1.6. - Miscellaneous

Our set-up will also allow us to study some additional feature on hyperon interactions. They can be summarized as follows:

(a) Study of the two and multiparticle correlation between the produced particles and in particular between strange and non strange particles.

(b) Study of the $\Sigma^- d \to p_s \Sigma^- \pi^- p$ and $\Xi^- d \to p_s \Xi^- p \pi^-$ reactions in order to investigate the virtual $\pi^- \Sigma^-$ and $\pi^- \Xi^-$ scattering.

2.2. Antiproton reactions

Apart of some rather low statistic experiments (1) not much information exists yet on $\bar{p}p$ interactions in the 100 — 250 GeV/c. One of the most interesting question arising in $\bar{p}p$ interactions concerns the presence of annihilation reactions at high energy. Based on the extrapolation of low energy data (10) and also on Regge exchange arguments one expects that the annihilation cross sections behaves as $\sigma_a(\text{mb}) = 61.8[P_{lab}(\text{GeV/c})]^{-0.6}$ (At 100 and 250 GeV/c for instance one would have a cross section of 3.9 and 2.3 mb, respectively). We propose to measure

the annihilation cross section as a function of the charged multiplicity in a momentum range of 100 – 250 GeV/c and also to investigate the production mechanisms (for instance to see if annihilation reactions are produced through central collisions as for low c.m. energies).

To this end we have to reject the non annihilation channel, i.e. :

$$\bar{p}N \rightarrow \bar{p}pX$$
$$\rightarrow \bar{p}nX$$
$$\rightarrow \bar{n}pX$$
$$\rightarrow \bar{n}nX$$

(where X means anything).

By means of the spot focusing we will be able to reject the events in which a leading $\bar{p}$ is emitted while the n or $\bar{n}$ will be detected by a neutron counter put downstream of the forward spectrometer (see Section 7).

For the annihilations and non annihilation reactions we also intend to study the statistical moments associated to the charged multiplicity distributions and to investigate their $\sqrt{S}$ dependence (for instance, KNO scaling). In particular, we would be able to see if the annihilation multiplicity distribution is narrower than for other type of hadron - hadron interactions (11). We also want to study the correlation between the average number of π^cs with the number of charged particleswhich will allow us to test various production models(12). Finally the study of resonance production is also envisaged.

3. GENERAL DESCRIPTION OF THE SET-UP

3.1. The set - up

The schematic representation of the experimental set - up is shown in Fig.1.1. The apparatus consists of a vertex detector coupled to a spot focusing Cerenkov counter followed by a downstream magnetic spectrometer.

The streamer chamber has a total gap of 40 cm and a sensitive volume of $120 \times 80 \times 40$ cm^3. Lead oxide plates are put inside the streamer chamber in order to detect outgoing π^o's. To obtain the magnetic field in the S.C. we would like to use the CERN 1m^3 heavy liquid bubble chamber magnet which has to be transformed in order to have a gap of 60cm with a field of at least 12 kG. We used for our various estimates the spectrometer configuration shown in Fig.1.1.

The gaseous targets (~100 atmospheres) will have a length of 30 cm and a diameter of ~ 5mm. The centre of this target will be placed at a distance of 25 cm from the beginning of the sensitive volume. In this way, we will see in the streamer chamber pictures 10 cm of the incoming beam track. This will be of great help for reconstructing in space the vertex of the interaction.

The downstream spectrometer consists of the following elements :

a). The spot focusing Cerenkov counter permits the identification of all the charged particles entering simultaneously in it, its geometrical acceptance being ± 10 mrad.

b). Superconducting coils of 1m diameter (20cm gap, 70cm aperture) already built, and two standard (or similar) P.S. magnets ($200 \times 20 \times 30$ cm^3)

c). A set of six planes of hodoscopes H_1 to H_6 used for the fast on line trigger. These hodoscopes are in the same planes as six sets of MPWC, PC_1 to PC_6 of high spatial resolution, but slower and therefore used only for the off line analysis. This system can detect Λ and also can follow the Y up to its point of decay.

d). A total absorption neutron counter used to reject $\bar{n}$ in the $\bar{p}$ part of the experiment, and which can detect Σ^- decays.

3.2. Performances

The present arrangement leads to a momentum resolution for the charged tracks shown in Fig.3.1. One sees from this figure that one has a momentum resolution which is always smaller than ~ 3 %. The errors calculated in the

streamer chamber with or without taking into account the fringe field and the lever arm were obtained from tracks with zero dip. For real tracks the errors will be slightly increased whenever the streamer chamber information will be used for measuring the momenta. When the momenta are determined by the additional magnets the errors are dominated by multiple scattering effects.
In this case however the overall errors can be decreased by using the redundant information on the track direction given by the spot focusing.

In order to calculate the acceptances of the various parts of our equipment as well as some other characteristics of our apparatus, we will consider the $\Sigma^- p \to \Sigma^- p \pi^+\pi^-\pi^o$ reaction. At 250 GeV/c this reaction was simulated by generating Monte-Carlo events according to the following matrix element squared:

$$|M_{if}|^2 \propto e^{bt_Y} e^{bt_p} \prod_{i=1}^{3} e^{-\alpha r_i^2} \qquad (1)$$

Here t_Y (t_p) is the four momentum transfer between the incident and outgoing Y(p) whereas r_i represents the transverse momentum modulus of the i-th outgoing pion. The above formula restores the leading particle effect as well as the limited transverse momentum behaviour of the outgoing particles.
The values of the slopes b and α were adjusted to agree with the single particle distributions obtained for pp interactions at 200 GeV/c (13). As furthermore, the generated pions lead to distributions which are very similar to real 200 GeV/c pn data (14) (Fig.3.2), the chosen $|M_{if}|^2$ is considered to give a rather realistic description of the $\Sigma^- p \to \Sigma^- p\pi^+\pi^-\pi^o$ reaction. This reaction will also serve us for the $\Xi^- p \to \Xi^- p\pi^+\pi^-\pi^o$ channel as practically no difference appears with the $\Sigma^- p \to \Sigma^- p\pi^+\pi^-\pi^o$ when they are generated with the same $|M_{if}|^2$. We obtain thus the momentum and angular distributions of the outgoing particles (Fig.3.3) as well as the x/r plot (Fig.3.4) expected for the outgoing π^o. These distribution will be used in order to calculate the various acceptances of our equipment.

Because of the geometry of the lead oxide plates in the streamer chamber (see Section 5) we will only be able to detect π^o's which are emitted in the laboratory with an angle $\theta > 9°$. Fig.3.4 shows that we will practically cover all of the backward hemisphere. In Fig. 3.5 we represent the acceptances of

the various parts of our equipment as function of the laboratory momentum of the outgoing tracks. One sees from this figure that the high momentum tracks will be accepted with a great efficiency by our downstream spectrometer. The good momentum resolution of these tracks (fig.3.1) is very promising for searching strange baryonic resonances. For instance for the $\Sigma^* \to \Sigma^{\pm}\pi^{\mp}$ resonances which will have a momentum of 200 GeV/c, we will obtain a mass resolution less than 13 and 23 MeV/c^2 for resonances having masses of 2 and 3 GeV/c^2, respectively.

3.3. The software

The software needed for analysing the events will be somewhat complex as one has to merge the information obtained from the streamer chamber and the downstream/upstream system. The upstream part will essentially be used for identifying and defining the incoming beam particles, while the downstream system will serve to identify and to measure the momenta of the outgoing particles. Both parts will of course be used in our triggering logic.

For handling the data we will take the approach developed now at CERN and which has proved its power for analysing the 30" hybrid system data (15). In the first stage of the treatment the streamer chamber information is used to determine the vertex position. Then one proceeds to the reconstruction of the tracks in the downstream system, constraining the tracks to pass through the previously determined vertex. At this stage the streamer chamber and downstream information are combined in order to link the tracks and to reject the spurious ones. An overall fit is then made in order to obtain the final geometrical reconstruction of the fast outgoing tracks. Finally the small momentum tracks which do not enter in the downstream spectrometer are reconstructed by using the chamber information only.

This technique has been applied successfully for handling the 100 – 200 GeV/c data taken with the 30" hybrid system. As an example we present in Fig.3.7 the momentum precision obtained from pd data at 200 GeV/c using this technique and conventional measuring machines in which the setting errors have been decreased. Note that for the present experiment we will obtain a better precision because of our additional downstream magnet.

In order to handle our data we intend to use essentially the new CERN software package (GEOHYB). Some transformation will of course be needed as we will

use a streamer chamber in which the vertex is not seen. Based on our experience in pn interactions at 200 GeV/c one can estimate the computer time needed for the full geometrical reconstruction of the events. For a six prong pn event (which corresponds roughly to the average charged multiplicity at 200 GeV/c) one needs a time which is about 2s of 6600 CP. We expect that this time will not be significantly increased by using our system in which the vertex is not seen on the picture.

4. THE HYPERON BEAM

A 250 to ~ 350 GeV/c hyperon beam must be built in the North Area with the following main specifications :

The beam design should follow the same basic principle (short length, high field dipoles, superconducting quadrupoles of very small aperture, beam particle identification with a special DISC in a "parallel" section) as the hyperon beam successfully built at CERN in 1970 (16,17,18).

In this section only the basic and minimal specifications are quoted, as the detailed beam design which represents a very sizeable effort is yet to be done. However in principle no new developments are needed in the design of the beam elements (dipoles and quadrupoles), as the ones designed and used for the pioneer beam at CERN - PS have proved their suitability and reliability from 1970 (19). The beam design is essentially a problem of computation for the optimisation of flux, momentum definition, background of muons, etc... We want to stress that the quality of the hyperon beam depends in a crucial way on the extracted proton beam emittance and halo, and has strong consequences on the beam design. Therefore experimental data on the SPS proton beam are essential to start the final beam design and we expect that in the near future they will be available.

1). The beam must be as short as possible. This requirement implies the use of superconducting beam elements of very small physical aperture (15 to 30 mm in diameter). The solid angle accepted in this beam must be at least 0.6 μSR which is not much less than the solid angle accepted by the beam lines under construction in the North Area.

2). The beam elements must image the production target on our H_2 target inside the streamer chamber. The "parallel" region where the DISC is inserted will be nearly achromatic. In the CERN - PS hyperon beam the angular dispersion at the DISC position was small but not zero. This was achieved by the proper sequence of polarity of the quadrupoles and dipoles. We don't require an exact achromatic beam because the DISC acceptance can be used effectively also as a mean to restrict electronically the total momentum bite of the beam. The cut in momentum obtained by the DISC can nicely complements the cuts introduced by the collimators installed in the beam channel and we want to keep this feature of the beam.

We expect that the monochromatic hyperon image can be not more than 0.5 mm in diameter (spot size at FWHM) and that the momentum dispersion be from ~ 0 up to 1.4 spot diameter per % in $\Delta p/p$.

3). The simultaneous identification of $\bar{p}$, Σ^-, Ξ^- and Ω^- is made with one multiplexed DISC counter placed in the parallel region of the beam channel.

4). The momentum definition of a beam particle is expected to be defined to about 1% with counter hodoscopes near the DISC and if necessary in front of the streamer chamber. It is important to notice that this 1% figure depends mostly on target size, determined by proton beam emittance, imperfections in beam element, and second orders effects.

5). The intensity of the 250 GeV/c Σ^- beam entering the streamer chamber target must be at least ~ 10000 Σ^-/burst. From the particle production spectra (20) it can be estimated that this flux should be reached with $\sim 10^{11}$ interacting protons at 400 GeV/c (see fig.4.1). This calculation has been made taking a $\Delta p/p$ of ± 1%, a solid angle of 0.6 μSR and a total beam length of 32.5 m. Moreover a 1.5 attenuation production factor has been included for the target efficiency compared to a H_2 proton target. The π^- contamination has also been estimated (Σ^-/π^- ~ 1%) and the number of π^- in the hyperon beam will be $\lesssim 10^6$ which is one of the requirements for the experiment.

It is worth noticing that the hyperon beam has even better performance between 250 and 350 GeV/c as shown on Fig.4.1. However event reconstruction and particle identification is more difficult the higher the momentum and this high energy part of the experiment is consequently left a priori for future runs.

On the contrary the $\bar{p}$ beam is useful only below 250 GeV/c. We intend to begin the experiment at ~ 130 GeV/c where the $\bar{p}$ flux and the $\bar{p}/\pi^-$ ratio are similar to the values estimated for Σ^- and Σ^-/π^- at 250 GeV/c, but with the advantage of requiring a 400 GeV/c proton beam reduced in intensity (~3 times less) and of making easier the identification of particles for testing the apparatus and starting the $\bar{p}$ experiment.

For the Ξ^-, the choice of 250 GeV/c momentum also looks a good compromise : the Ξ^- flux on the H_2 target is maximum around 250 GeV/c for a 400 GeV/c primary beam. This estimate is based on the Grote - Hagedorn - Ranft calculations for the shape of the curve but normalized by scaling from 24 GeV/c CERN Data (21) and 25.8 and 23.4 GeV/c BNL Data.

The flux of background muons tolerable in the streamer chamber ($\sim 0.5\ m^2$ in cross section) is estimated to be ~ 1 per μsec.

Our proposed hyperon beam being refocused to a spot is only slightly longer 32.5 m than the hyperon beam proposed at FNAL 29.5 m (elastic scattering of the hyperons, addendum to E97. Proposal #497, May 13, 1976 by C. Ankenbrandt et al.)

We contemplate to use higher gradient quadrupoles of smaller aperture, and shorter DISC which accounts for the small difference in total beam length. Our beam configuration can be expected to give higher beam purity and better background conditions.

It is supposed that this beam can be installed in E H N 1, derived from an attenuated primary proton beam transported to the production target by one of the existing beams for example H_2 or H_4. The total length of the hyperon beam + experiment should be 60 to 70 m.

5. THE STREAMER CHAMBER AND VERTEX MAGNET

The vertex detector will be a detecting He-Ne streamer chamber with a H_2 high pressure gas target installed as shown in fig. 5.1. The size of the chamber fits in an existing magnet (the N P A magnet built for the CERN heavy liquid bubble chamber). A modification of this magnet will however be necessary in order to increase the gap from 20 to 60 cm and to provide a rectangular hole at the top (60 x 180 cm^2).

The visible volume of the streamer chamber will be 120 x 120 x 40 cm^3.

This chamber is complementary to the spot focusing and consequently must fulfill special requirements. This is the reason why a particular arrangement has been chosen for this square streamer chamber. It is fed with the high voltage pulse from the top of the magnet and matched to its characteristic impedance at the bottom. This position will allow to minimize the amount of material put into the beam line and will provide a large forward angular acceptance (vertical $50^o \pm 4^o$, horizontal $19^o \pm 1.5^o$) with a very small amount of matter ($\sim 5 \times 10^{-3}$ radiation length including the gas itself). Moreover the access to the target side will be easier and counters and MWPC can be installed close to the chamber on both sides.

We have chosen for the chamber the twin geometry proposed by Rohrbeck et al., (22).

This arrangement is particularly convenient when a target must be installed in the chamber because it provides an ideal position for the target which can then be installed exactly in the central section of the chamber where no matter is present (no high voltage plane). Background interactions and flares are consequently reduced in comparison to what can be observed with the conventional double gap strip line geometry.

The target itself will be made of a thin tube (about 5 mm in diameter), 30 cm in length, filled and flushed with H_2 at very high pressure (typical 100 bar). With the expected beam intensity about 60 interactions (Σp) will be obtained in the hydrogen target for $\sim 10^6$ π^- created at the target

production ~ 32.5 m upstream. We will also get ~4000 pion interactions per burst. The percentage of interactions outside the target in the various windows will be about 30%. The incoming hyperon will be visible over 10 cm in the streamer chamber before entering the H_2 target. This will provide an off-line information for positioning the vertex of the interaction and could also be used to confirm that the incident hyperon is within the momentum bite. It also gives a signature that no interaction has occured between the DISC and the H_2 target. Due to its large width and small gap the wave impedance of the streamer chamber cell is low ($Z_o = \sim 12\ \Omega$ per channel). This value is about half the average impedance of usual streamer chambers. Particular care will then be taken in order to maintain the rise time of the high voltage impulse at a low value ($< \sim 4$ nsec). We have already achieved a 1.3 nsec rise time in a 25 Ω chamber (23). We consequently are quite confident that a 3 to 4 nsec rise time can be achieved in the new proposed chamber following a similar design but with a strip line geometry.

The quality of the darts is better the smaller the pulse length τ (23), but the peak field $\hat{E}$ at the onset of the streamers increases with τ decreasing ($\hat{E} \propto \tau^{-1/3}$). A good compromise between quality and technological difficulties is to choose about 7 nsec FWHM pulse for a He-Ne mixture. With this kind of pulse duration positive and negative ~ 210 kV pulses must feed the chamber. To generate these positive and negative pulses a twin Marx generator will be built using the existing CERN-COGECO 100 kV, 10 nF condensors which will guarantee a high reliability at a minimum cost.

The optical system will consist of 3 cameras and image intensifiers (I.I.). The film will be 50 mm of the non perforated type. Taking into account the resolution of the optical system (limited mainly by the I.I. at ~ 30 ℓp/mm) and a demagnification of ~ x 40 the radius of the reprojected darts in space will be ~ 650 μm giving a two-tracks resolution of ~ 1.5 mm. The expected setting error is ≤ ~ 250 μm in space.

Like for all streamer chambers a number of interesting characteristics can be pointed out for this streamer chamber (for more complete discussion see ref. (24)).

5.1 Precision of measurements

In spite of its modest length (typical: 1 m tracks) and a large setting error (∿ 250 μm) the precision on the momentum is below 2% for all momenta (for 1 m track and 12 kG) up to 5 GeV/c and then increases slowly with p ($\left(\frac{\Delta p}{p}\right)_{\%} = 0.40\ p_{GeV/c}$ for no dip). At very low p values (100 MeV/c) the precision is still good (< ∿ 2%) because of the low mass of the vertex detector (long range and low multiple scattering). For the same reasons the errors on angles are also small (< 1 mrad for p > ∿ 1 GeV/c).

5.2 Ionization measurement and identification

With a track length of 80 cm it is possible to measure the specific primary ionization of a particle in a large range of γ values $\left(\gamma = \frac{p}{\beta m}\right)$ from ∿ 1.3 to ∞ with a precision of ∿ 8% (25) in a He-Ne mixture (70 - 30%) set at 1μsec memory using traces of SF_6 (23).

Slow particles can be identified using the strong β^{-2} dependence of the ionization in this range (fig. 5.2).

Above minimum (γ > 4) the relativistic rise of the ionization up to 50% (at γ ∿ 200) allows some identification between π and K,p which are separated by more than 8% ionization difference (23% p/π and 14% for K/π but only ∿ 8% for p/K).

Using a HPD system it has been showed (25) that ∿ 4 pictures/min can be digitized and fully analyzed, the ionization measurement (streamer counts) is automatically included in this analysis.

It is also possible to detect γ's in a large fraction of the solid angle around the target and then to get some information on π^o production by inserting a cylinder made of lead-oxide (one radiation length ∿ 2 cm) into the visible volume of the chamber as shown in fig. 5.1.

5.3 Range and target cuts

The range for protons is given in fig. 5.3 in H_2, He and He-Ne 30-70% (by volume) mixture. The range is ∿ 230 times longer in this He-Ne mixture than in a liquid H_2 bubble chamber.

With the 5 mm diameter target filled with 100 bar H_2 gas the momentum cut for recoiling protons is $\sim$ 115 MeV/c ($\sim$ 70 MeV/c for π). At 200 MeV/c a proton looses only $\sim$ 10 MeV/c in the target before becoming visible in the streamer chamber. A 200 MeV/c π looses less than 1% in momentum in the same target.

It is also intended to use other kinds of targets: solid, liquid or even the gas of the streamer chamber itself if very low t values must be studied ($t \sim 0.001$ $(GeV/c)^2$ for p) or if a visible vertex is required. The interaction rates will still be high enough in that case to get one interaction picture per pulse.

5.4 Background sensitivity, time resolution, triggering sensitivity and data acquisition rates

At very high energy it is clear that background problems must be studied carefully. For a hyperon beam the problem is even more serious because the primary proton target is not far from the vertex detector in order to minimize the hyperon loss through decays.

In this respect, due to its short and adjustable time resolution (from 0.5 µsec up) and its low mass, the streamer chamber is a good instrument. Up to 10^6 - 10^7 μ/m^2sec flux can easily be accepted with no loss in event reconstruction. In the beam acceptance itself it is also possible to accept a few 10^6 charged particles per second without loosing detection efficiency.

In the Table 5.1 we give an estimation of the necessary triggering characteristic for the expected 10^4 Σ^-/burst beam as a function of the kind of target put in the chamber. The triggering sensitivity is defined as the fraction in percent of the total cross section Σ^- + N on which we have to trigger the chamber in order to get one picture per pulse.

5.5 The vertex magnet

The 100 tons NPA magnet (26) after its modification in 1964 for fitting the 1182ℓ HLBC had a usefull gap of 20 cm and was working up to a horizontal magnetic field of 27 kG with a power dissipation of 4.5 MW.

We propose a modification of this magnet in order to increase this gap from 20 to 60 cm. As we wish to introduce the chamber from the top of the magnet we also require a clearance hole of 60 x 180 cm^2 in the top plate.

The magnetic field must be at least 12 kG in the whole volume of the chamber with good homogeneity.

We wish to photograph from one side in a plane perpendicular to the central magnetic field and then require a free hole of 130 cm in diameter.

We have estimated work, cost and time duration implied by these modifications:

(a) Machining of old pieces and $\sim$ 26.5 tons of iron and $\sim$ 5.6 tons of stainless steel to add, disassembly and re-assembly of the magnet, water connections, power supply to re-start, measurement of the field.

(b) $\sim$ 650 kSF in $\sim$ 28 months.

(c) $\sim$ 2.5 MW at 12 kG.

6. SPOT FOCUSING DETECTOR

One essential aspect of this proposal, is the presence of a SPOT FOCUSING DETECTOR used as a trigger and for the particle identification in the forward cone.

Although such an instrument is only in its development stage at C E R N it is basically a natural extension of the DISC counters which have been created in this laboratory. Presently a prototype is being built to solve some of the problems connected with the use of multichannel plate phototubes and small PM sensitive to the single photoelectron which were not yet available and have delayed so far this detector.

The DISC counters are essentially "yes" or "no" detectors which accept a particle when it is in a very well defined narrow range of velocity and angle with a certain direction, and ignore all other particles. Their use is in the tagging of our particle at a time in a secondary beam or in a spectrometer. They are very fast and can handle very intense beam, $\lesssim 10^7$/sec, and they have very high rejection, $\sim 10^6$ against unwanted particle. This can be achieved with a fast electronic and a small number of high quality phototubes (typically 8).

On the other hand, the SPOT FOCUSING DETECTOR (SF) is a Cerenkov detector optically corrected like a DISC, and can collect simultaneously the information on the velocity (or gamma), and on the angle of many particles emitted simultaneously from an interaction vertex. It is clear that much more information is extracted per event than from a DISC and therefore the SF requires a much larger number of photodetectors, this explains the need for the new Multianode Channel Plate Multiplier developed by Philips , or the very small PM, made by Hamamatsu.

Sample of both types of detectors have been obtained and are being tested at C E R N and we are confident that suitable photo detectors for a S.F. will be available in the near future.

In the prototype SF most of the parts have been delivered, except for the special optical elements which will be delivered soon.

We are already in the position to design the S.F. to which we refer in this proposal provided that the tests of the prototype are successful and to bring it in operation with the predicted performances with the same confidence we have had in the design of DISC counter, i.e. within a definite time scale and budget.

6.1. Properties of the Spot Focusing(27)

The S.F. detector consists in a vessel containing a gas in which the downstream charged particles produce Cerenkov Radiation in the near U.V. In our case the vessel is 6m long, the entrance window is at 2m downstream from the interaction vertex, and it contains a Nitrogen + Helium mixture at atmosphere pressure.

The windows will be of minimal thickness, and there is no particular safety problem.

The particles are emitted from the interaction vertex in a volume of about 2mm in diameter and 300mm in length and at an angle $< \pm 10$ mrad. They will radiate a Cerenkov light cone wich is sharply focused onto a spot for a given value γ_0 of γ and onto a circle for $\gamma \neq \gamma_0$. As an example γ_0 can be set to ∞ and the range of detection extends from $\gamma_{min} = 80$ (cf. see below) and $\gamma_0 = \infty$ of course any value of γ_0 can be set according to the setting value chosen for the pressure. The position of the spot, on the centre of the circle corresponds to the emission angle of the particle. The radius φ of the circle is related to γ according to

$$\varphi = \frac{\text{EFL (equivalent focal length)}}{2\gamma^2 \theta_0}$$

the equivalent focal length of the system EFL is adjustable between 20 and 60 m, θ_0 is the Cerenkov angle for which there is spot focusing.

By focusing all the Cerenkov light on a point (about 20 photoelectrons), i.e. on our single photodetector element, the pattern recognition problem is reduced to a trivial one. A spot is a unique signature of a charged particle of a definite γ_0 (as it gives a pulse of high amplitude on one or at most four adjacent photodetectors), and a p_T given by the distance of the photoelement from the center of the matrix. Therefore the S.F. can be used as a trigger on a selected forward particle of a given mass, and p_T. This is valid even if many other charged particles are emitted simultaneously in the forward cone. The particles having a γ distinct from the γ_0 corresponding to the pressure of the counter, will produce circles on the photodetector matrix, most of them with an amplitude corresponding to a single photoelectron and will be easily rejected by the trigger electronic. An off line treatment of the pattern of light recorded on the photodetector matrix and will

provide with the gamma, the emission angles, and the multiplicity of the particles of each event. Even a coarse momentum analysis will be sufficient with the S.F. data to identify the mass of each particle. As there is no dead regions in a S.F., and as the light intensity is far above the threshold of detection of the photodetector matrix, the detection efficiency is essentially 100% for all the particle in the γ range of the S.F. set by the condition that a sufficient fraction of the ring image fall on the photodetector matrix even at the maximum divergence angle. Of course particles below the Cerenkov threshold ($\gamma_T = 57$ for $\gamma_0 = \infty$) produce no light at all, and are absolutely ignored by the S.F. This can be an aid in particle identification with the S.F.

We expect, exactly as observed in DISC counters, and for the same reasons, that delta rays produce blurred Cerenkov ring, and are not accepted by the pattern recognition process.

6.2. Description of the SPOT FOCUSING DETECTOR

We propose to build a S.F. detector which will rely heavily on the design of the elements of the prototype S.F.

The optical correction will be based on the same principles as in the prototype. The axiconic corrector doublet can be manufactured with flat external optical surface, and a full correction of the chromatism (apochromatic correction) for a particular combination of indices of refraction for the corrector element (fused silice and H^20), and for the gas radiator, (Nitrogen with Helium admixture)). The gas pressure can be set to one atmosphere when using the proper gas mixture, alleviating the need for a thick window and a costly gas vessel.

The 6 meter long vessel contains the gas radiator at atmospheric pressure. At the downstream end the main spherical mirror has a radius of curvature $R_M = 8000$ mm and a diameter $\phi_M = 375$ mm, is positionned with its centre of curvature at the vertex position. A free space of about 2 meters is available between the vertex and the entrance window of the S.F. detector. The main mirror can be thinned out a circular central region of $\emptyset = 160$ to a residual thickness of about 5 mm of glass. Therefore the particles in the forward cone $\alpha \leq 10$ mrad will see 6 meters of N_2He at atmosphere pressure + about 1 gr/cm^2 of glass and window material.

Particles at $10 \leq \tau \leq 25$ mrad, will see the full thickness of the mirror, i.e. about 10 gr/cm^2.

Particles at $25 \leq \tau \leq N$ 50 mrad, pass only through the gas and the thin windows until they reach the limits of the steel vessel, set at 50 mrad for a $\phi = 800$ mm vessel.

The light reflected from the main spherical mirror goes back at the upstream end of the detector where it is reflected by a plane mirror wich has a central hole, on the axiconic corrector and focusing lens which are fixed on an extension of the vessel at 30° to the beam axis.

Light is focussed by this optics on the matrix of photodetector placed (in the case we have to use small phototubes which are six times larger than the elements of the Philips tube, requiring therefore a larger optical magnification) at 24 to 69 meter from the S.F. detector. The matrix of small PM is about one meter in diameter.

6.3. Matrix of photodetectors

The photoelectrons yields $\overline{N}$ for particle is given by

$$\overline{N} = AL\Theta^2 = 0.184\,A$$

We can expect with the near U.V. transmission of the optics to reach A = 100 for small phototubes or for the channel plate multianode phototube of Philips. A spot on a single photoelement of about 18 photoelectrons is an excellent signal. But for particles having $\gamma \neq \gamma_0$, the same number of photoelectrons is distributed on many photoelements, and therefore in order not to loose information, it is required that each photodetector be sensitive to a single photoelectron. This is achieved in an excellent way by the multianode of Philips. A prototype of this tube has been manufactured for an evaluation, it has 25 elements, and the tests were very successful, to the exception of its lifetime which is shortened by the degradation of the photocathode to an unacceptable level (about a day of run).

The specialists of the LEP laboratory, the Philips development lab, are well aware of this problem and we have to wait for their progress. Meanwhile a larger version of this tube is being studied by LEP, with a much larger number of anodes (some hundreds of them).

The size of a photoelement is nearly immaterial for a S.F. detector. The light pattern is magnified by a transfer lens to match the pixel size, and matched simultaneously to the γ resolution and the angular field of view.

If LEP cannot produce early enough an acceptable multianode detector, the S.F. detector can be fitted with more conventional miniature phototubes. Hamamatsu has provided us, with a 14 mm diameter tube which is being tested and exhibits the performances we need for this application.

The electronics is the same in both cases. In the future the cost of the Philips tubes is still unknown, it may be competitive with the cost of the small phototubes (365 SF for the Hamamatsu tube).

The matrix of photodetectors is the main cost of the S.F. detector, and its performances are directly related to the number and to the cost of the photoelements.

Therefore it is possible to trade performances against cost.

The ultimate optical resolution of the S.F. for a photoelement size ϕ_{PM} divided by the equivalent length $F_M G$ is equal to the angular spread of the focussed Cerenkov light $\Delta\theta$ = 100mμ/4m = 25.10^{-6} radian corresponding to a velocity resolution

$$\frac{\Delta\beta}{\beta} = \theta\,\Delta\theta = 17.5\ 10^{-3} \times 25\ 10^{-6} = 4.4\ 10^{-7}$$

This resolution is similar to the C E R N NAL DISC and corresponds to a

$$\frac{\Delta\gamma}{\gamma} = 4.4\ 10^{-3} \text{ at } 100 \text{ GeV/c}$$

The actual resolution we will obtain in an experimental situation is worse for two reasons :

(a). The photodetector matrix will be coarser for cost reasons,

(b). The transverse dimension of the vertex (target diameter 2a) produces a blurred spot (Nuclear Instruments and Methods III (1973) 397-412, "A spot focusing Cerenkov counter for the detection of multiparticle events at High energy" , M. Benot, J.M. Howie, J. Litt, R. Meunier

An approximate formula for $\frac{\Delta\gamma}{\gamma}$ is

$$\frac{\Delta\gamma}{\gamma} = \frac{\beta\gamma^2\theta}{F_M}\left[\frac{a}{2} + \frac{\phi_{PM}}{G}\right]$$

F_M is the main mirror focal length. G is the optical magnification.

The field of view is given for a circular matrix of photodetector as

$$\tau = \pm\sqrt{\frac{N}{\pi}}\,\frac{\phi_{PM}}{F_M \cdot G}$$

The following table indicates $\frac{\Delta\gamma}{\gamma}$ for two matrices of different cost.

γ		80	100	200	290
N° 1	$\frac{\phi_{PM}}{G}$ = 2.24 mm (1000 photoelements)	$\frac{\Delta\gamma}{\gamma}$ = 7,6%	11.9	47.6	100%
N° 2	$\frac{\phi_{PM}}{G}$ = 1 mm (5000 photoelements)	4.2	6.5	26.2	55

The N° 1 corresponds to a matrix of 36 photoelements on a diameter (about 500 mm in diameter with 1000 Hamamatsu phototubes). The N° 2 corresponds to 80 photoelements on 1.12 meter diameter, and 5000 elements.

In both case ± 10 mrad are covered.

The minimum $\gamma_{min} = 80$ quoted corresponds to a γ for which when the S.F. is set to focus a spot for $\gamma = \infty$, the circle on the matrix is of a diameter equal to the radius of the matrix. The Cerenkov angle is 12.5 mrad be for γ_{min}, the photoelectric light yield is halved, and for a particle emitted at 10 mrad, only half the ring image will fall on the matrix. This value of γ can be considered as the minimum gamma for about 100% detection efficiency.

The maximum γ, $\gamma_{MAX} = 290$ is the highest value for which the spot focused can be recognised as being larger than our pixel, for a matrix of 36 elements on a diameter. This is still adequate to recognise a proton from a pion.

6.4. Particle mass identification

The mass of the particle is known from its momentum p and its γ.

$$M = \frac{p}{\beta\gamma}$$

We have approximately

$$\frac{\Delta M}{M} = \frac{\Delta p}{p} = \frac{\Delta\gamma}{\gamma}$$

$\frac{\Delta\gamma}{\gamma}$ has to be better than 10% only in the difficult case where one wants to separate Σ^- from Ξ^- ($\frac{\Delta M}{M}$ = 10%) and better than 25% for the $\bar{p}\Sigma^-$ separation ($\frac{\Delta M}{M}$ = 25%).

For all the other cases, to the exception of a separate identification of π, μ, e, $\frac{\Delta\gamma}{\gamma}$ can be as high as 50%.

6.5. Electronics

The specific property of the Cerenkov light is its isochronism on the photocathode when focused, even when the path in the radiator is many meters in length. The light is a practical delta function without any afterglow. Therefore the Cerenkov light signal is ideal, it shows no dead time, no memory, and no pile-up. The electronics is straightforward. The pulses given by each photoelement are treated in parallel in fast electronics and after a passive delay reach a gate which is an equal plane in time, that can be set in coincidence with the other counters in the beam. The light pattern on the matrix will be stored on magnetic tape for off-line analysis. The dot pattern gives the charged multiplicity for the particle above γ_{MIN}, their γ and their emission angle in the solid angle acceptance of the S.F., where tracks cannot be well separated in the S.C. pictures.

The angular accuracy is :

$$\Delta\tau = \frac{1}{2F_M}\left(\frac{a}{2} + \frac{F_M}{G}\right) = \pm\ 0.34 \text{ mrad, case N° 1}$$
$$= \pm\ 0.18 \text{ mrad, case N° 2}$$

and is obtained off-line, at the same time that a fit is performed on the ring size, and position.

It is not irrelevant to mention a unique property of the S.F. detector. In the special case of the particles (not necessarily of the same mass) coming from a cluster, they all have nearly the same γ. The S.F. can be tuned to focus all of them to a spot making the search for correlated particles particularly simple, and this process can take place on line as it requires only fast electronics (no off line fitting).

Most of this electronics is a straightforward adaptation to the large array of phototubes of the wire chamber read out electronics, which has been built for many SPS experiments on a similar scale.

7. TRIGGERING AND NUMBER OF EVENTS

In order to carry out our physics program we will use different trigger arrangements. In all these arrangements we will use the Disc in the beam line facility to identify the incident particles and a set of scintillator counters in order to define a beam profile with a small cross section. This requirement of an incoming beam focused on a target of very small radial dimension is a feature of the experiment. The essential characteristics are :

1). The interaction vertex is already physically constrained in space (within ± 1 mm in radial position).

2). The wall of the high pressure target is minimised allowing low momentum particles to recoil and to be analysed in the streamer chamber (momentum for proton ~ 115 MeV/c).

3). In a hyperon beam there is no possibility to install a conventional momentum slit as this would require a considerable extension of the beam length. The next best thing which we can do is to let the momentum dispersed beam interact with a small target in order to restrict the accepted momentum band down to 2 to 3 %.

4). A small target is an essential requirement of the spot focusing detector.

The basic principles of the trigger are as follows :

1). In order to run efficiently the trigger rate must :

- match the data taking rate of the streamer chamber (1 to ~ 10 per sec.)
- be highly selective for events corresponding to the interaction of a Y or and $\bar{p}$ in the target and very insensitive to background
- be loose enough and not requiring necessarily a particular configuration of the event. This condition insures the experiment of an unbiased acquisition of data, and makes the "S.C.S.F." (streamer chamber - spot focusing) combination similar in this respect to a bubble chamber experiment.

2). Nevertheless the interaction trigger can also be restricted to more specific signature of the event with the different counters we have at our disposal. For example a matrix of scintillators covering the downstream end of the S.C., can indicate the presence of charged particles associated with an

interaction in the target. A neutron counter detects the Σ^- decays. This counter can also be included in the trigger.

3). The trigger pulse for the S.C. is obtained from the following signals :

1.- The Disc in the beam, specific signature of a $\bar{p}$, Σ^-, Ξ^- (Ω^-)

2.- The beam defining scintillator counters (position and momentum determination)

3.- The S.F. analysing the forward particles coming out from the interaction vertex. One large pulse in a photodetector (or few adjacent) is a signature of a particle of a certain γ_0 (adjustable with the gas index) emitted at a certain angle. Even if the particle is the same as the incoming beam particle, the requirement on the angle indicates that there has been an interaction in the target and not only a straight through beam particle.

4). Six planes of hodoscopes along the downstream spectrometer. As the interaction vertex is physically constrained to the target, any particle emitted from it with a momentum high enough to be accepted in the downstream spectrometer must cross the different hodoscopes at coordinates entirely specified by particle momentum and emission angle and accurately known through the charged particle transfer matrices of our magnetic channel. For a particle tagged by the S.F. its mass is also known.

We intend to bring the pulse of every counter to a fast multiple coïncidence system which will compare the hit pattern with a stored pattern of acceptable events. This system can be made fast and easily adaptable to the various experimental cases. This interaction trigger can have high efficiency because all the detectors involved for triggering are scintillation counters with essentially 100 % efficiency, and Cerenkov counters (90 to 95 % efficiency).

However a high rate of ambiguous events is generated by the decays in flight of the hyperons, not only from the Σ^- and Ξ^- but also from the Λ. The MPWC associated with the hodoscopes planes have an order of magnitude better resolution and can therefore resolve off - line many ambiguities. We adopt as a reasonable estimate that not more than 50 % of our triggers can lead to fully analysed events.

a). Hyperon physics

To study the semi-inclusive reactions $YN \to \Sigma X$, ΞX, ΩX one has to identify the outgoing hyperon. If one does not require an accurate measurement of the hyperon momenta, the Y has to survive only until the end of the spot focusing. Using the interaction trigger and requiring that one charged particle at least will pass through the spot focusing we will obtain the event rates given in Table 7.1 for a 1 mb cross section. We also give in Table 7.2 estimates of some typical cross sections with the corresponding number of events/day which we will obtain. By requiring that the hyperon will survive until the end of last magnet one remains with a reduced number (although still appreciable of events/day). The trigger condition is now a coincidence between the interaction trigger the spot focusing and the hodoscopes H_1 to H_6 (Fig.1.1). Most of the events which have decayed between the hodoscope MWPC, can be recovered.

The decay pions has a large momentum difference with respect to outgoing Y, hence the decay of the hyperon will be detected by our system. The Fig.7.1 shows the momentum spectra of the π^- coming from the decay of Σ^-, Ξ^- or Ω^-.

b). $\bar{p}$ annihilation physics

In order to study the $\bar{p}p$ and $\bar{p}n$ annihilation reactions, one has to reject the events having a nucleon/antinucleon in the final state. This rejection will be made by means of the spot focusing an a neutron counter put downstream of our spectrometer. In fact the neutron counter will be calibrated during the run using the fact that the $\bar{p}p \to \bar{p}nX$ and $\bar{p}p \to \bar{n}pX$ cross section have to be equal. The $\bar{p}p \to \bar{p}nX$ reaction will be identified with the spot focusing and separated from the $\bar{p}p \to \bar{p}pX$ by observing the streamer chamber pictures. Indeed for $\bar{N}pX$ final states the outgoing p will have a momentum smaller than 1.5 GeV/c (the momentum of the outgoing proton in the $\bar{p}N \to \bar{N}pX$ reaction is not expected to be different from that obtained in the $\Sigma^- p \to \Sigma^- p\pi^+\pi^-\pi^o$ reaction, see Fig.3.3) and could hence will be easily recognized by ionisation (see curves in Fig.5.2). By the same method the $\bar{n}pX$ final state will be separated from the $\bar{n}nX$ ones.

c). Multiplicity distributions as function of the atomic weight of the target

This study will be made with incident $\bar{p}$, Σ^-, Ξ^- particles using essentially gaseous target (see Table 7.3) and an interaction trigger.

For the $\bar{p}$ beam the multiplicity study will be made as a function of the incident momentum in the range of 100 to 250 GeV/c. Beam flux, annihilation cross section and maximum number of events per day are shown on Table 7.4.

8. CONCLUSIONS

We present here a new instrument very powerful and flexible for studying multiparticle production at the SPS energy at minimum cost. In fact the proposed instrument is an outcome of many developments made at CERN in particle detectors during in the last decade. In addition one has to emphasize that our instrument will be able to bring an original and significant contribution to the hyperon multiparticle production and $\bar{p}$ physics.

We can make same considerations about this facility :

1). Each separate part of the system can be operational for physics and the facility can be brought up by steps.

For illustration the starting up of the beam alone with its identification, and the accurate measurements of particles production would already be an experiment by itself. We do not mention it, as we think that by the time the beam is ready, FNAL results will be available. An hyperon elastic experiment similar to E 497 could also be effectively performed at CERN with only the beam and the S.C.S.F.

2). As far as efficiency of the facility is concerned we may state that the data acquisition rate is from 1 to 10 pictures + electronic data on particles momenta and on identification, per accelerator spill.

3). Provided that the incoming beam can be focused in a small target, this facility can study, with a specific trigger, interactions induced by particles that we cannot produce in separated beams.

8.1. Cost and requirements from CERN

In order to carry out our experiment we would like to use the EF streamer chamber with its associated equipment. However a new streamer chamber body has to be constructed for the present experiment and an additional high voltage power supply has to be provided. In addition the CERN $1m^3$ heavy liquid bubble chamber magnet has to be transformed in order to have a field of at least 12 kG with a gap of 60cm. As these equipments could also be used as a CERN new facility for other experiments we would like to ask from CERN to finance the cost of these modifications as well as the construction of the spot focusing system (see Table 8.1a) and of the hyperon beam in the North Area. We ask CERN to design and build the proposed beam and to study the shielding

and safety problems. The collaboration intends to finance all of the equipment which is specific to our experiment. Table 8.1b indicates the cost foreseen for the equipment provided by our collaboration.

8.2. Manpower, data analysis and running time

For the time being 25 physicists will participate in the proposed experiment. The participation groups have already counter and hybrid bubble chamber experience in the study of interactions in the 100 – 300 GeV/c incident momentum region. The groups of Bari and Strasbourg are participating in several experiments at Fermilab.

For the construction of the equipment we will dispose of our workshops and in particular those available at Bari and Strasbourg. The software needed to treat the data will be developed by Strasbourg.

All the groups have scanning power, and about 30 scanners (half-time) will participate in this experiment. To measure the events we will use an HPD (Strasbourg), the CRT from IN_2P_3 located in Paris VI and conventional measuring machines in which the setting errors have been decreased by means of a television camera.

The data reduction will be done with the computer available in Bari (IBM 370-175) and in Strasbourg (UNIVAC 1110). We propose to divide our physics programme in 4 successive phases starting with the Σ^- physics. In Table 8.2 this programme is shown together with the number of required events and the computer time is estimated for the analysis of the data.

A period of about 3 years is envisaged for design and construction of the beam and of the apparatus.

REFERENCES

1). There exist some low statistics $\bar{p}N$ experiments made primarly with the Fermilab Hybrid Bubble Chamber. See for instance : R. Ansorge et al., Phys. Letters 59B, 299 (1975)

2). H.J. Lipkin, Fermilab - Conf. 75/79 - THY

3). C. Quigg and J.L. Rosner, Phys. Rev., D14, 160 (1976)

4). Multiparticle production in $\bar{p}$ induced reactions, A. Fridman, to be published in the Proceedings of the Antiproton - proton Symposium, Stockholm (1976)

5). S. Barshay et al., Phys. Rev. Letters, 32, 1390 (1974)

6). H.J. Lipkin, Phys. Rev., D7, 846 (1973)

7). G. Cohen-Tannoudji, J.M. Drouffe, P. Moussa and R. Peschauski, Phys. Letters, 33B, 183 (1970)

8). Assuming factorization one can get an estimate for the double diffraction dissociation cross section from $\sigma_{DD} \leqslant \sigma_D^2/4\sigma_{el}$. By using available data on p dissociation at 150 GeV/c one obtains $\sigma_{DD} \sim 0.3$ mb.

9). R.D. Tripp, Proceedings of the Int. Conf. on High Energy Physics, Vienna (1968) p.173

10). CERN/HERA Report 73-1, 1973

11). S. Barshay, A. Fridman and P. Juillot, Strasbourg preprint (PN/HE 75-15) to be published in Phys. Rev.

12). See for instance ; F.T. Dao and J. Withmore, Phys. Letters, 46B,252 (1973)

13). See for instance : J. Withmore - Phys. Reports, 10C, May 1974

14). Data of the Strasbourg - Weizmann Collaboration

15). F. Bruyant, GEOHYB program development at CERN

16). R. Meunier, Charged hyperon beam, Memorandum to E.E.C., 23.4.1969

17). R. Meunier, Charged hyperon beam, Memorandum to E.E.C., 27.6.1969, PH I/COM-69/32

18). J. Badier et al., Hyperon beam experiment, Memorandum to E.E.C., 30.10.1969

19). M. Marquet, M. Morpurgo, Cryogenics 11 (1971) 412

20). Grote - Hagedorn - Ranft, Particle spectra, CERN 1970

21). J. Badier et al., Phys. Letters, 39B, 414 (1972)

22). W. Rohrbeck and G. Bohm, Int. Report, Zentralinstitut für Elektronenphysik der Akademie der Wissenschaften der DDR - 1973

23). F. Rohrbach et al., Hydrogen streamer chamber up to atmospheric pressure, Preprint CERN/EF/76-2

24). F. Rohrbach, Characteristics of a vertex streamer chamber, CERN/EF 76-1

25). I. Derado et al., Search for "charmed" mesons and baryons in high energy collisions with a streamer chamber vertex spectrometer CERN/SPSC 76-62 Add.2 (p.37)

26). G. Patak, Electro-aimant de chambre à bulles, Bulletin Oerlikon, N° 346/347, p. 70-78 (196)

27). M. Benot, J.M. Howie, J. Litt and R. Meunier, A spot focusing Cerenkov counter for the detection of multiparticle events at high energies, Nucl. Instr. and Meth., III (1973) 397 - 412

TABLE 5.1 Trigger sensitivity for different type of targets, using 10^4 Σ^-/burst

	30 cm liquid H_2	30 cm 100atm H_2, 15°C	1 m, latm H_2, 15°C
Interaction length Σ^- 150 GeV/c	∿ 6.3 m	∿ 52 m	∿ 5.2 km
Number of Σ + N int. per pulse per $10^4\Sigma^-$ inside the target	∿ 479	∿ 58	∿ 2
number of corresponding π interactions (~ 10^6 π) inside the target	∿ 3.2 x 10^4	∿ 3.8 x 10^3	~ 130
percentage of interactions outside the fiducial target [16] in various windows	∿ 30%	∿ 30%	∿ 70%
Trigger sensitivity for 1 evt/picture	∿ 0.16%	∿ 1.3%	∿ 37%
Detector sensitivity for Σ^-+p physics in evts/μbarn day for 10 000 bursts/day (∿ 20h, 7sec cycle)	∿ 128	∿ 15	∿ 0.5

TABLE 7.1 - Estimation of the number of events/day induced by hyperon induced reaction with hydrogen for a 1mb reaction cross section. Here $Y_{SF,DS}$ denotes the outgoing hyperon, the indices SF and DS denoting that Y survives until the end of the spot focusing or the downstream spectrometer, respectively (X means anything)
The Ξ^- beam intensity is taken as 500 per 10^{11} interacting protons

Reactions	$\Sigma^- p \to Y_{SF} X$	$\Sigma^- p \to Y_{DS} X$	$\Xi^- p \to Y_{SF} X$	$\Xi^- p \to Y_{DS} X$
Number of events/day for a 1 mb cross section	2600	640	140	30

TABLE 7.2 - Estimates of some typical cross sections and number of events expected per day

Reaction	Estimated cross section (mb)	Number of event/day
$\Sigma^- p \to Y^*_{SF} p$ (1)	0.3	780
$\Sigma^- p \to Y^*_{DS} p$ (2)	0.3	190
$\Sigma^- p \to Y^*_{SF} X$ (3)	0.9	2340
$\Sigma^- p \to Y^*_{DS} X$ (4)	0.9	580
$\Sigma^- p \to Y^*_{SF} \bar{\Lambda}\Lambda X$ (5)	1.5	7 (with the 2Λ decaying in the chamber)
$\Sigma^- p \to Y^*_{SF} \bar{\Lambda}\Lambda X$ (6)	1.5	170 (with one Λ decaying in the streamer chamber)

The cross section were estimated in the following way. For reaction (1) and (2) we assumed that $\sigma(\Sigma^- p \to Y^* p) = \sigma(pp \to N^*(1680)p)$ where Y^* is assumed to be the SU(3) partner of the N (1680). The cross section for (3) and (4) were obtained from factorization arguments. In (4) and (5) we assumed that Λ production is as numerous as in pp interaction at 150 GeV/c ($\sim$ 3mb). We assumed then that $\sigma(\Sigma^- p) \to \Sigma^- \Lambda\bar{\Lambda}X) \simeq 3/2$ mb.

TABLE 7.3 - Gaseous targets which may be used for the study of multiplicity distributions as a function of the atomic weight A of the target. The cross sections σ(pp) are taken from the Review of Particle Properties, April 1976 Edition. We also plane to use some solid targets as for instance carbon (A = 12.01).

Gas	A	$\delta(0^{o}C)$ gr/l	σ mb
H_2	1.01	0.09	39
D_2	2.01	0.18	74
He	4.00	0.178	134
N_2	14.01	1.25	390
Ne	20.18	0.90	520
A	39.95	1.78	890
Kr	83.80	3.71	~1600
Xe	131.30	5.85	~2200

TABLE 7.4 - Number of expected $\bar{p}$/burst entering in the streamer chamber and $\bar{p}/\pi^-$ ratios. In all these cases we used 10^6 particles/burst as the total number of particles entering in the streamer chamber

Incident momentum (GeV/c)	100	150	200	250
$\bar{p}$/burst	$1.5\ 10^{4}$	$8\ 10^{3}$	$3.6\ 10^{3}$	$2\ 10^{3}$
$\bar{p}/\pi^-$	$1.5\ 10^{-2}$	$0.8\ 10^{-2}$	$0.4\ 10^{-2}$	$0.2\ 10^{-2}$
Annihilation cross section (mb)	3.9	3.1	2.6	2.3
Number of events per 10^4 BURST (~ per day)	$9.5\ 10^{4}$	$4\ 10^{4}$	$1.5\ 10^{4}$	$0.7\ 10^{4}$

TABLE 8.1a - Cost of the financial effort we are asking from CERN
(The cost of the beam is not included)

ELEMENT	COST (KSF)
Streamer chamber body + high voltage	300
Transformation of $1m^3$ HLBC magnet	650
Spot focusing + Data acquisition	800
T o t a l	1750 KSF

TABLE 8.1b - Cost estimate of the equipment provided by the collaboration

ELEMENT	COST (KSF)
Neutron detector	150
Hodoscopes	100
Multiwire proportional chambers	300
Cryostat for the coils	150
Associated electronics	200
Trigger logic	200
Camera support	50
Image intensifiers	300
Cameras	100
T o t a l	1550 KSF

TABLE 8.2 - The different phases of the proposed experiment.

Phases of the experiment	Physics to be studied	Number of required events	Computer time for CDC 6600 needed for the analysis (hours)
A	Σ^-N reactions	2×10^5	340
B	Ξ^-N reactions	2×10^5	340
C	$\bar{p}$ annihilation	1.2×10^5	200
D	Multiplicity as a function of A $\bar{p}$ (100 to 250 GeV/c) Σ^- (250 GeV/c) Ξ^- (250 GeV/c)	 8×10^4 2×10^4 2×10^4	small

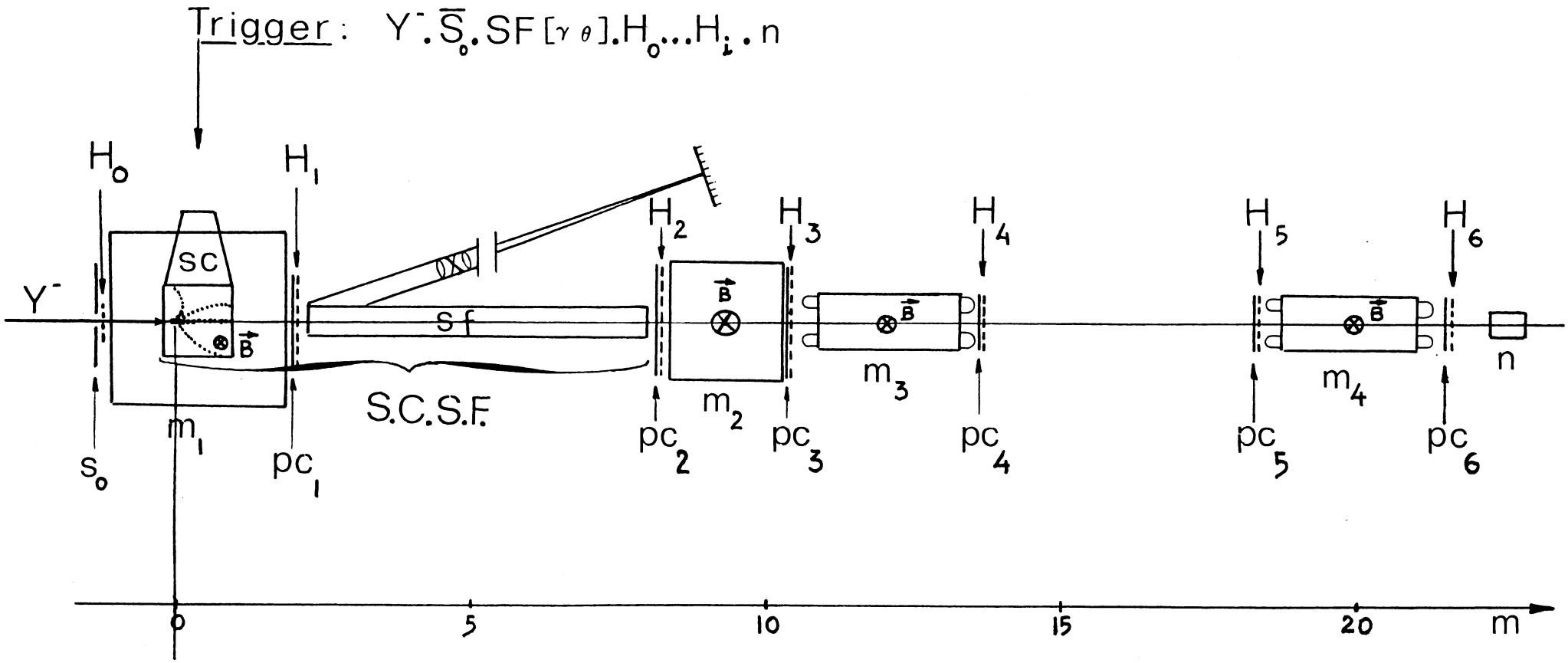

Fig.1.1 Schematic representation of the S.C.S.F. spectrometer (Side view)

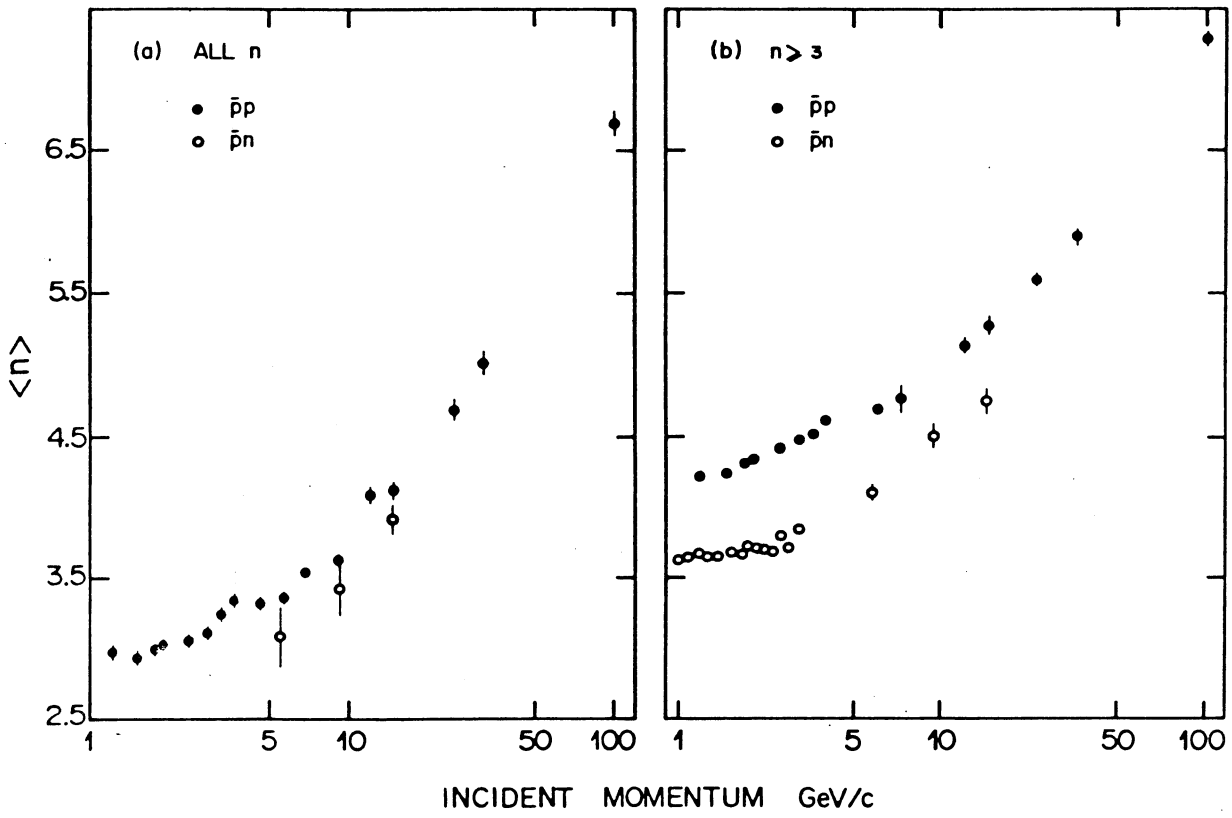

Figure 2.1

(a) Comparison between the average multiplicity for $\bar{p}p$ and $\bar{p}n$ interactions

(b) Same distributions as in (a) but obtained from multiplicity distributions when the number of charged particles is $n \geq 3$.

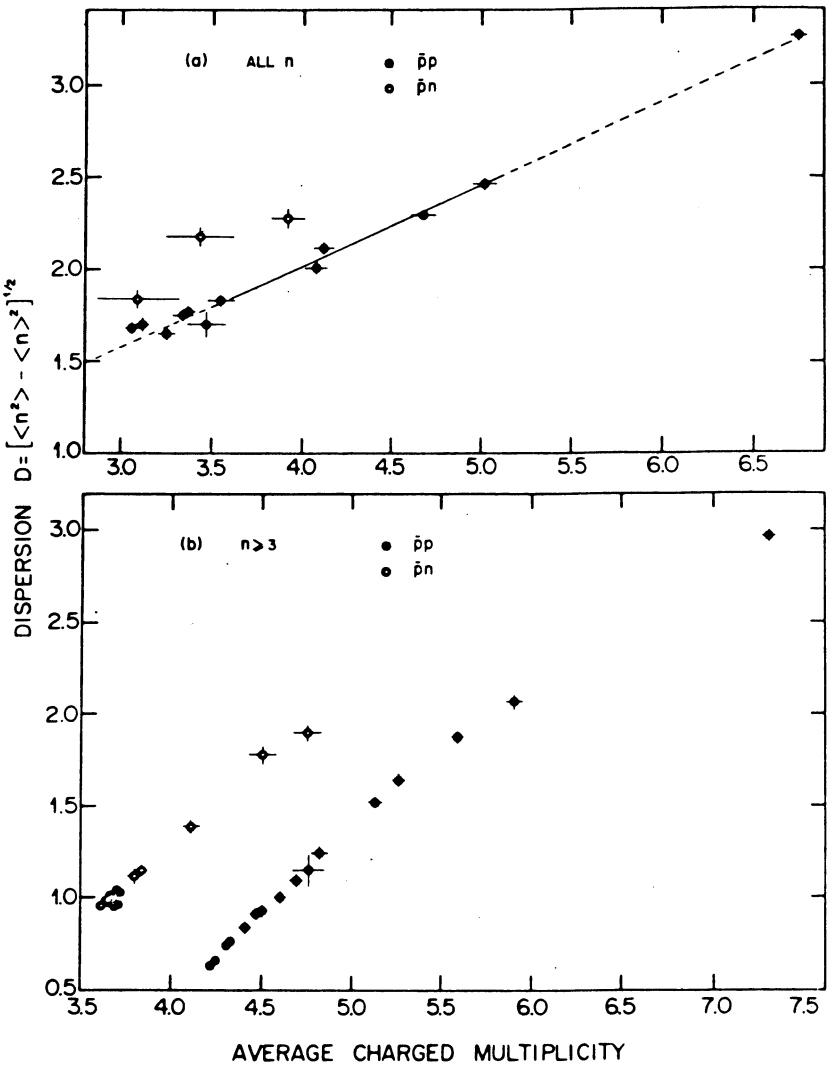

Figure 2.2

a) The dispersion D of the charged multiplicity versus its average <n> for $\bar{p}p$ and $\bar{p}n$ interactions. The full line represents a linear fit to the data in the $3.5 < <n> < 5.5$ region. By including the 100 GeV/c point one obtains $D = [0.44 \pm 0.02]<n> + [0.27 \pm 0.05]$.

b) The same distributions as above but obtained from multiplicities with $n \geq 3$.

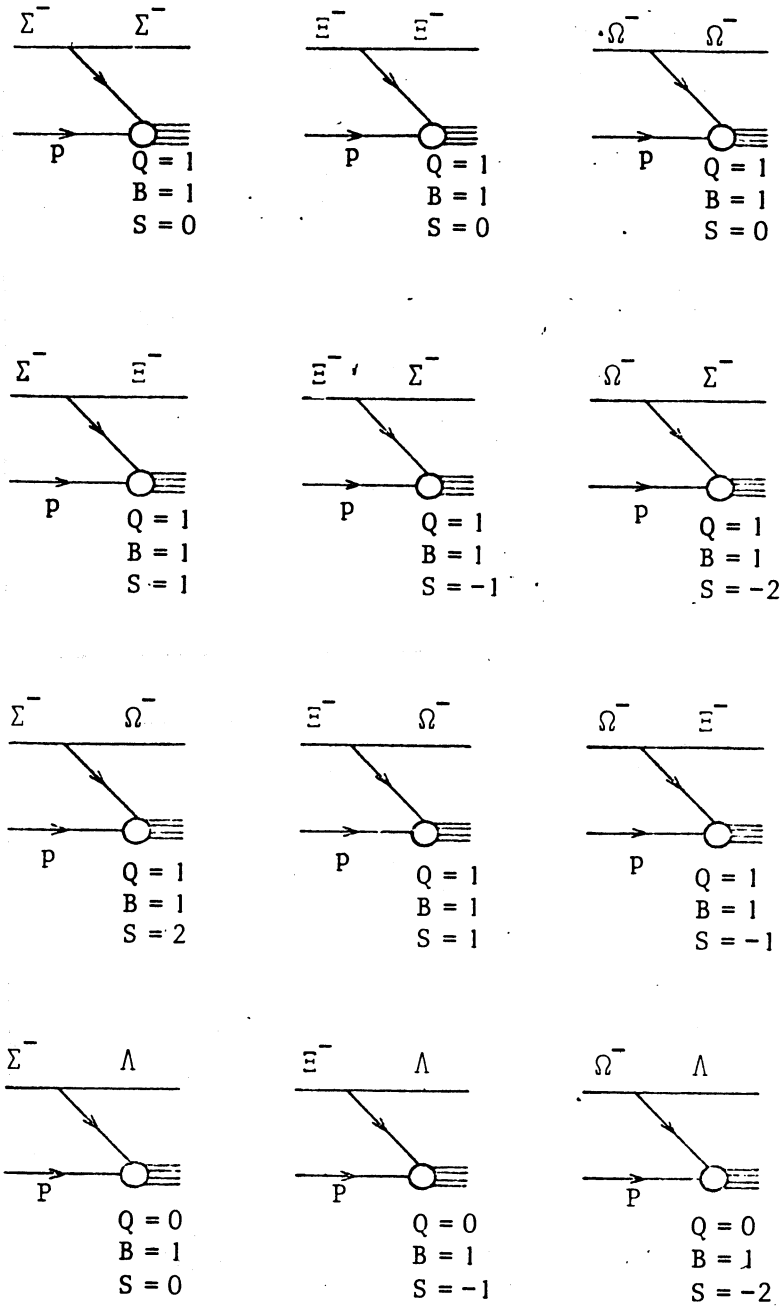

Fig.2.3 Examples of recoiling systems produced with definite quantum numbers. By using a neutron target all the charges will be decreased by one unit. Other possibilities can also be considered as for instance two particles emitted forward. One can also search for processes with baryon or exotic exchanges in the t-channel.

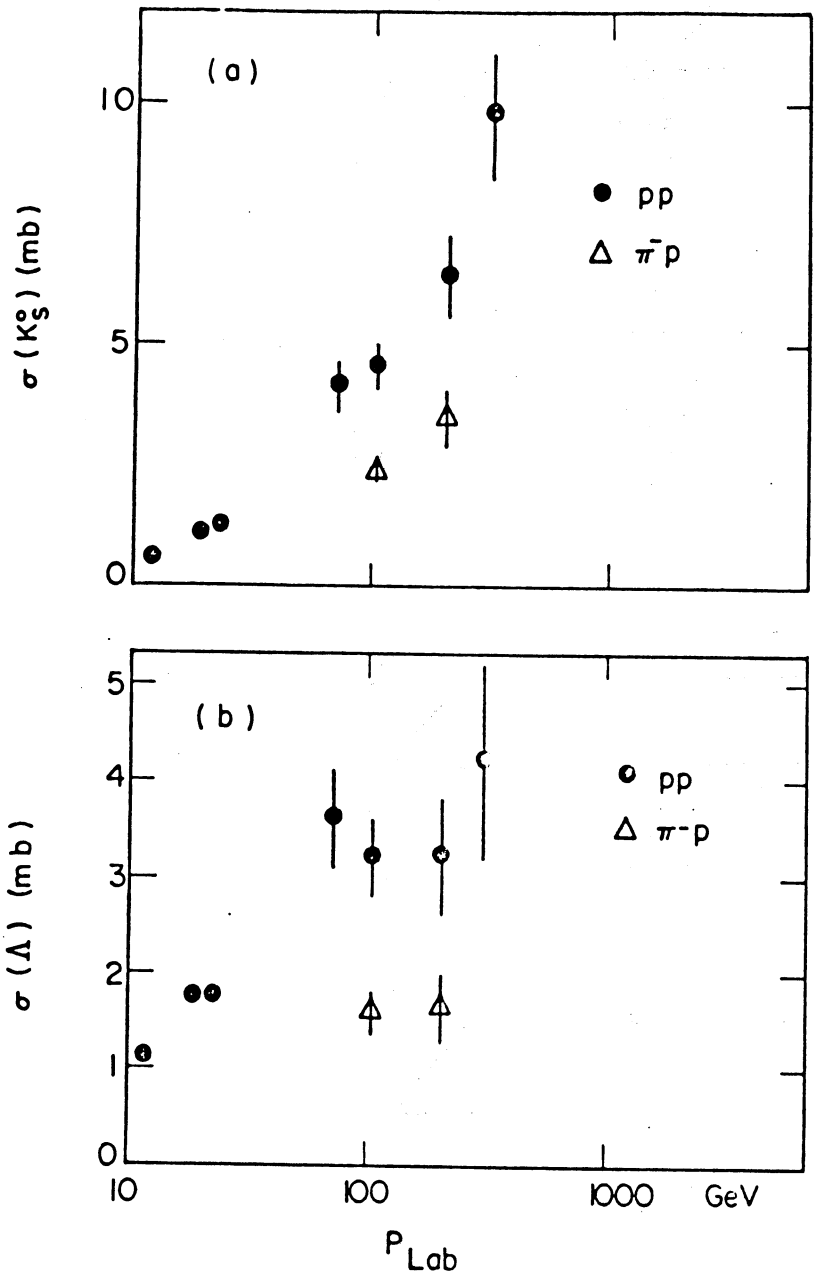

Fig.2.1

Fig 2.4. Cross sections for strange particle production at high energies

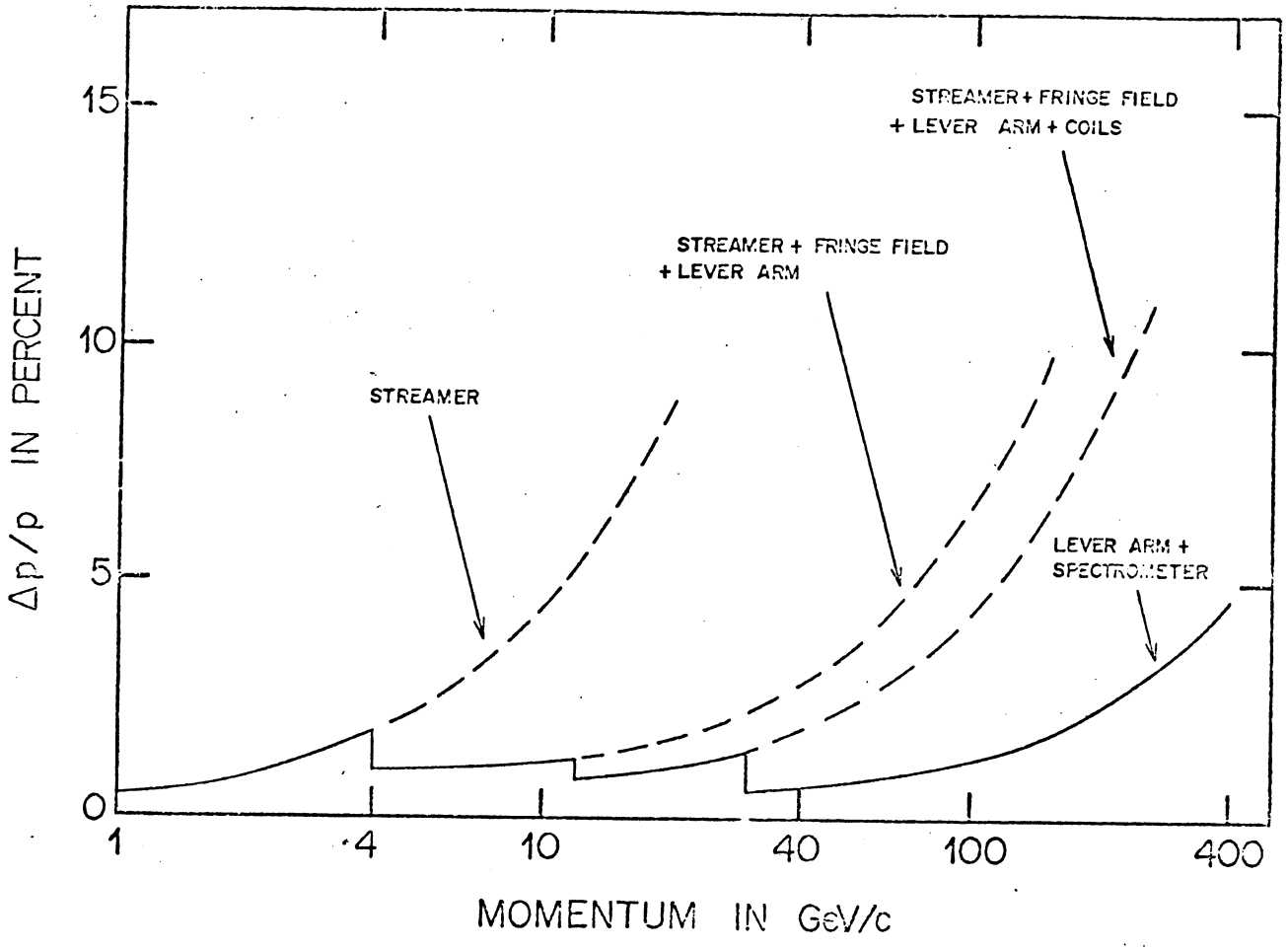

Fig. 3.1 Percentage error on the momentum of zero dip outgoing tracks

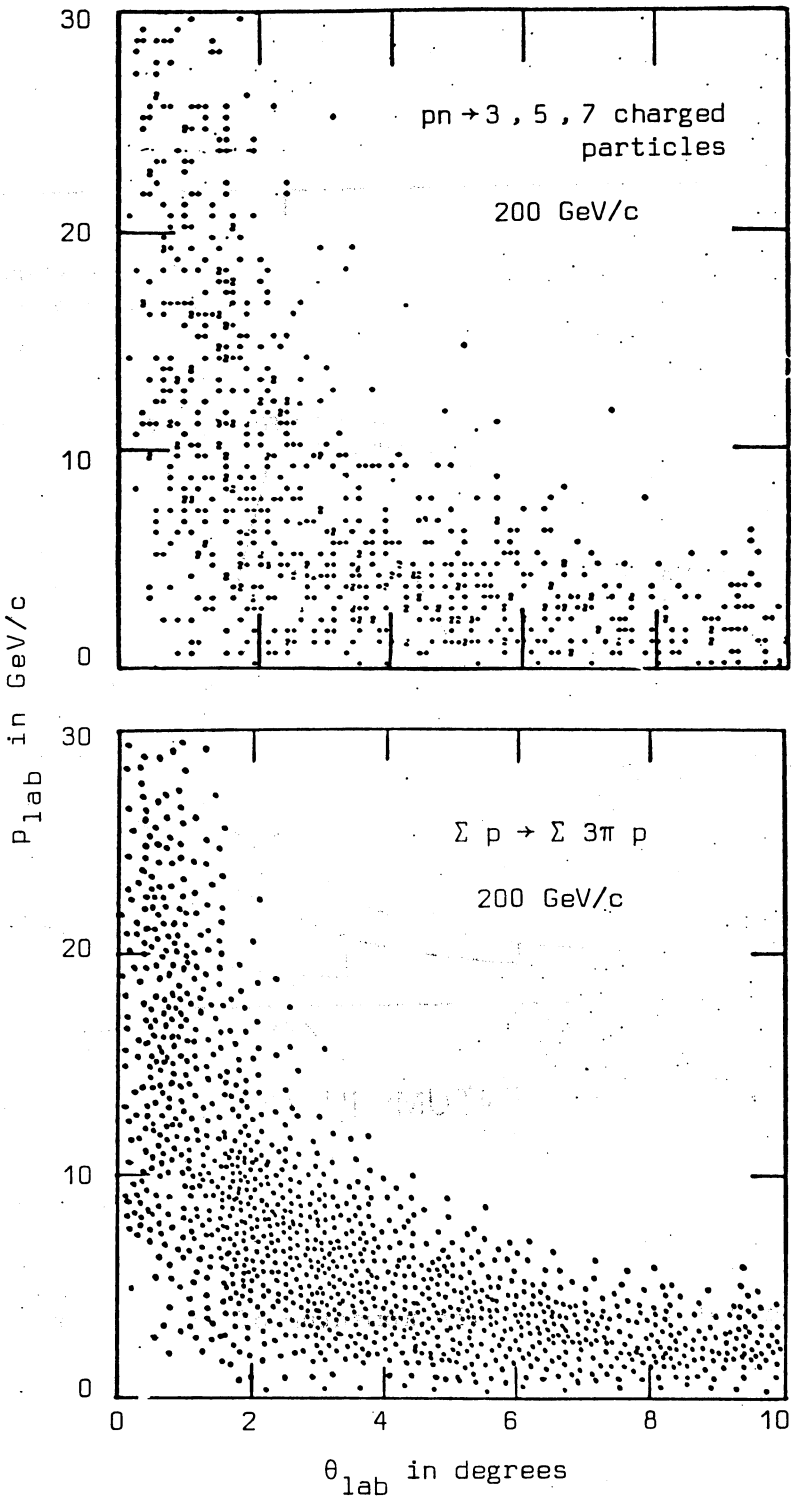

Fig 3.2 Scatter plot of the emission angle θ_{lab} versus the momentum p_{lab} in the laboratory system ,

a) For negative particles in three, five, and seven charged particle final states of pn reactions at 200 GeV/c.

b) For pions of $\Sigma p \rightarrow \Sigma\ 3\pi\ p$ faked reaction at 200 GeV/c .

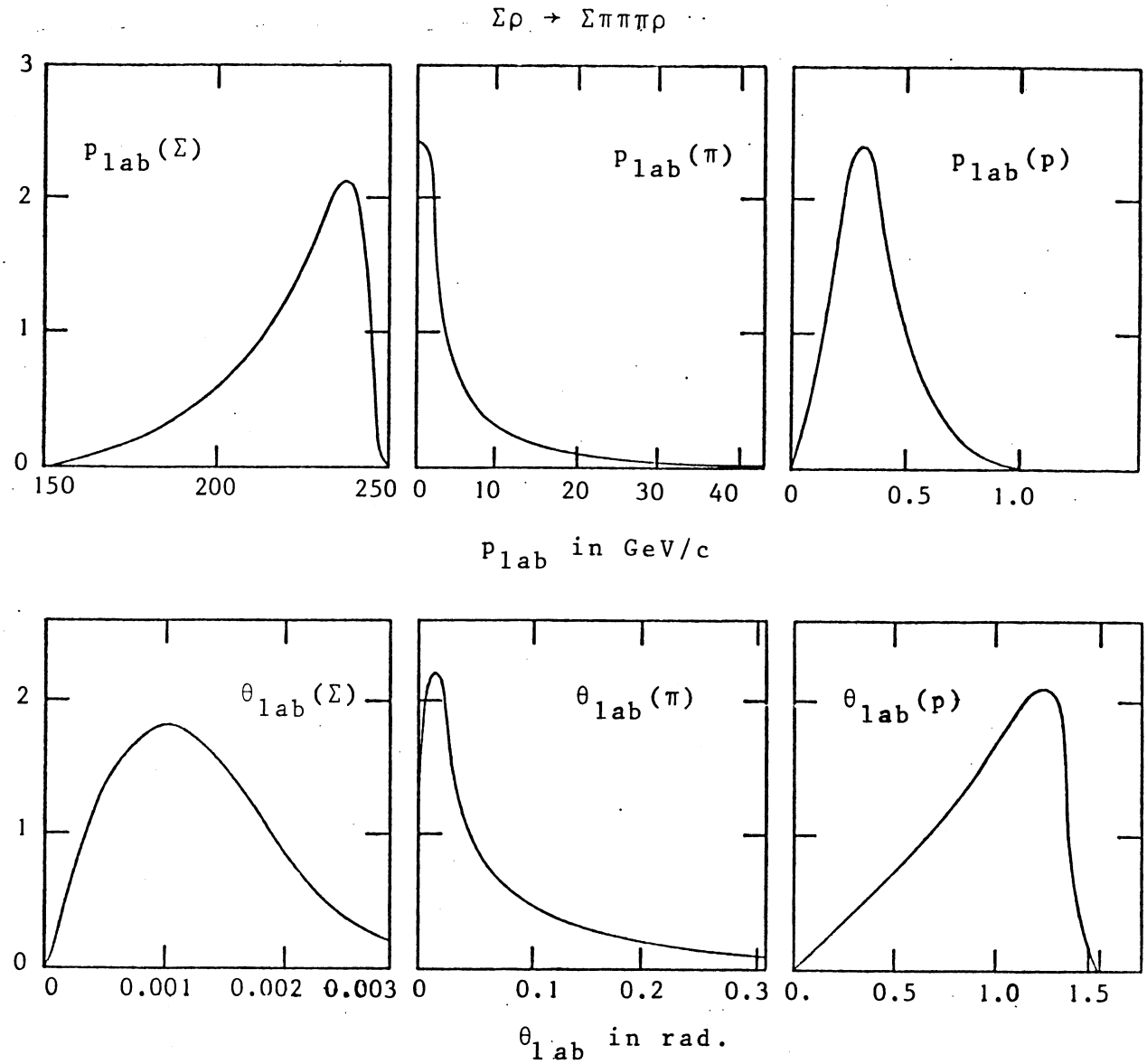

Fig. 3.3 Momentum and angular distribution of the outgoing particles obtained by generating peripheral events. These events will be used to calculate the various acceptances of our apparatus.

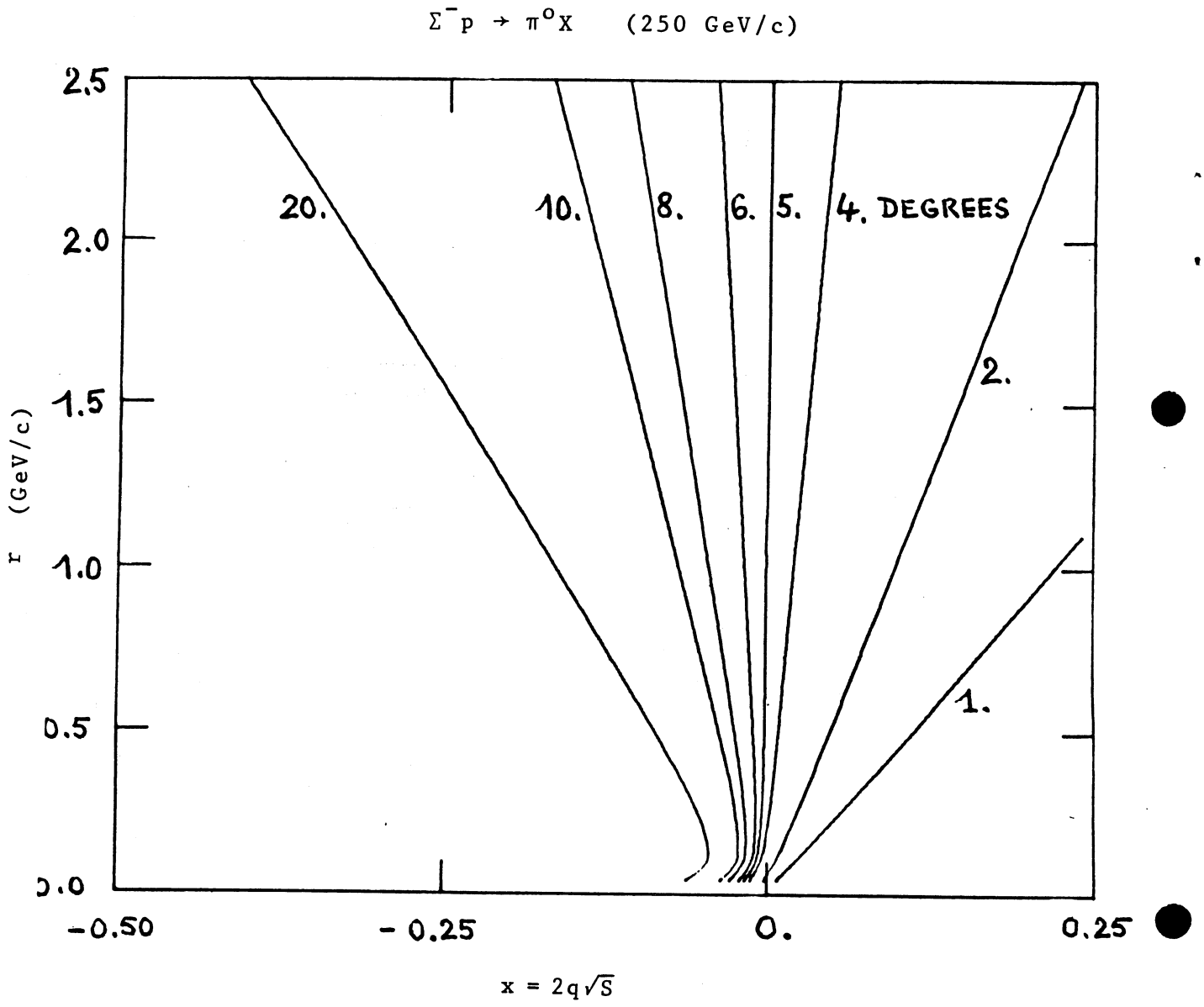

Fig.3.4 Lines of constant emission angle for the π^o in the $\Sigma^- p \rightarrow \Sigma^- p \pi^+ \pi^- \pi^o$ reaction at 250 GeV/c in the r versus x scatter plot. Here r is the transverse momentum of the π^o and x its Feynman variable. Note that by detecting π^o with an emission angle greater than 9° one accords most of the π^o produced in the backward c.m. hemispheres.

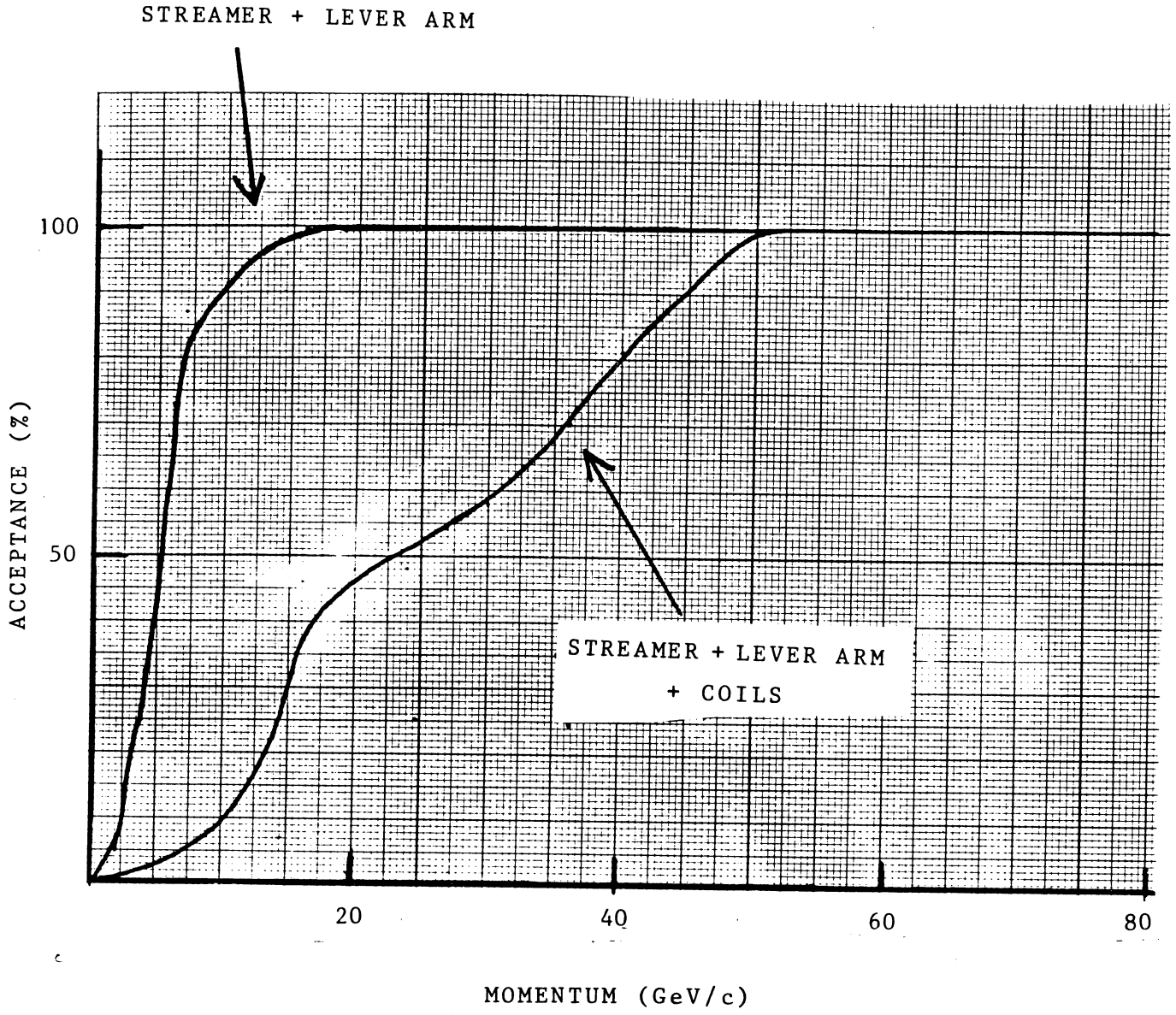

Fig. 3.5 Acceptance of the charged pions by the two first multiwire proportional chamber (streamer + lever arm) and by the superconducting coils (streamer + lever arm + coils). Practically no π are accepted by the last chamber while its acceptance for the leading particles is 94 %.

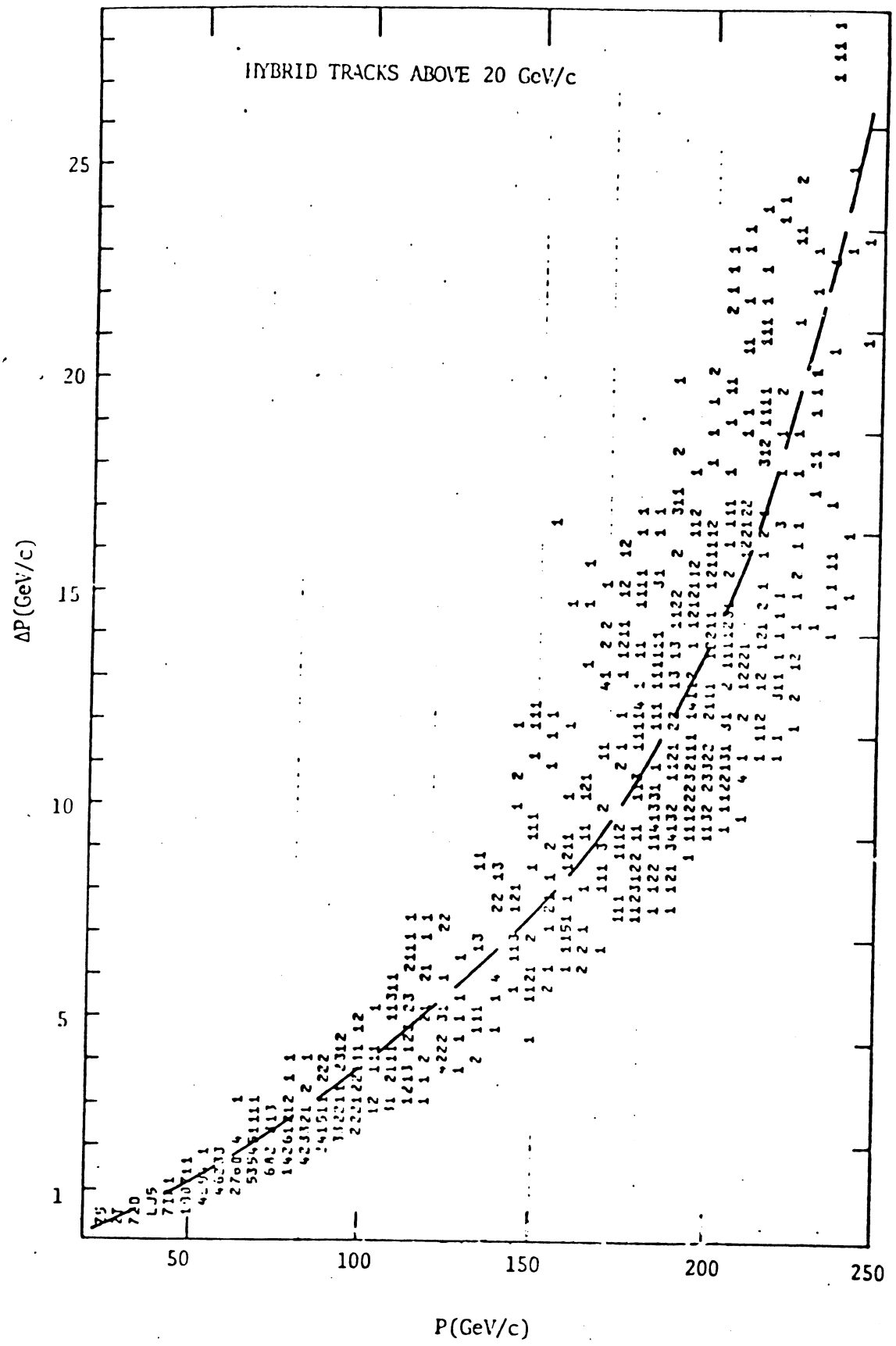

Fig. 3.6 Momentum precision obtained from pn data at 200 GeV/c taken with the 30" hybrid system. The tracks were measured with the modified Strasbourg conventionnal measuring machines.

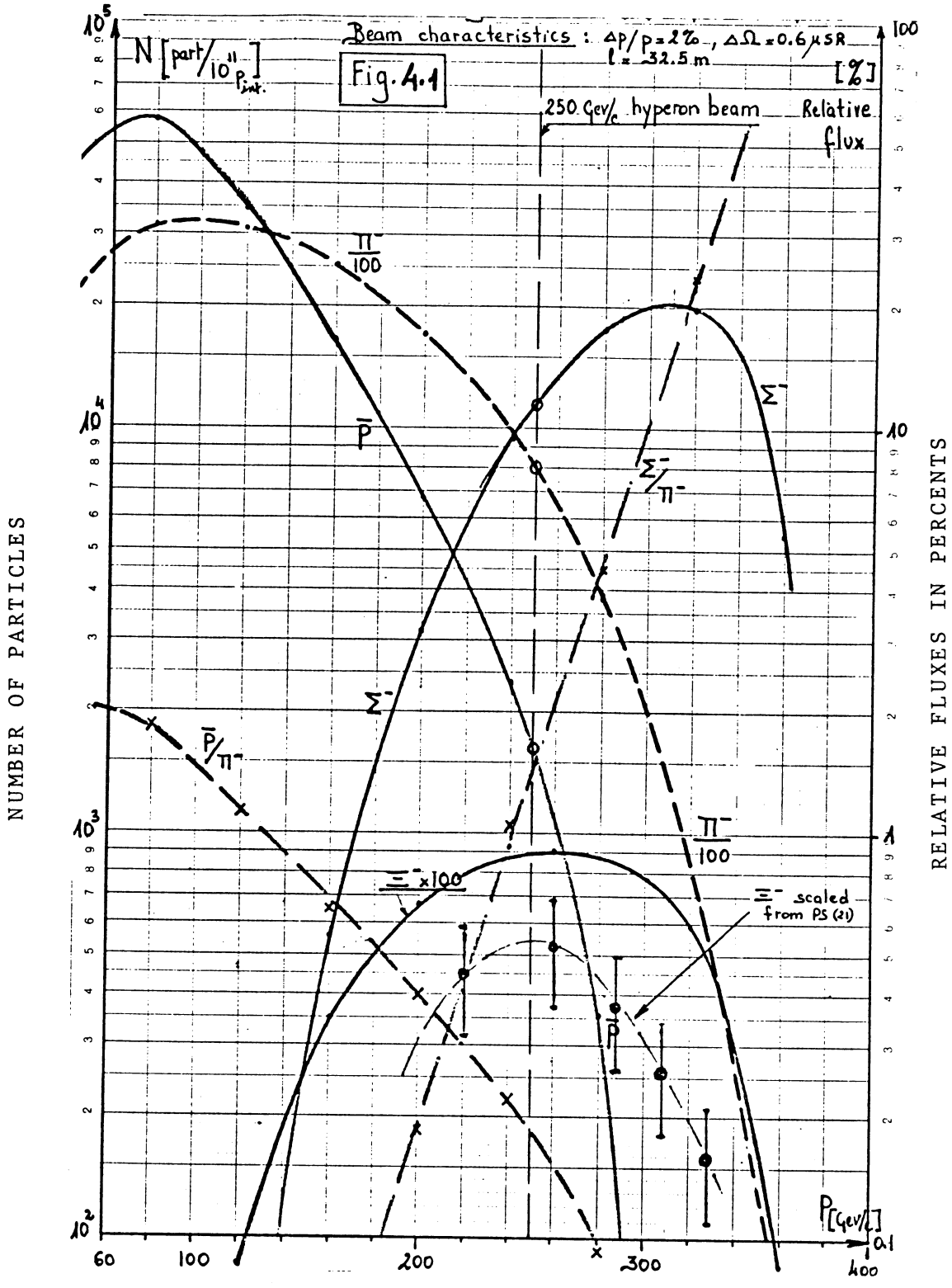

Fig.4.1 Number of particles at the streamer chamber target/10^{11} interacting protons at 400 GeV/c.

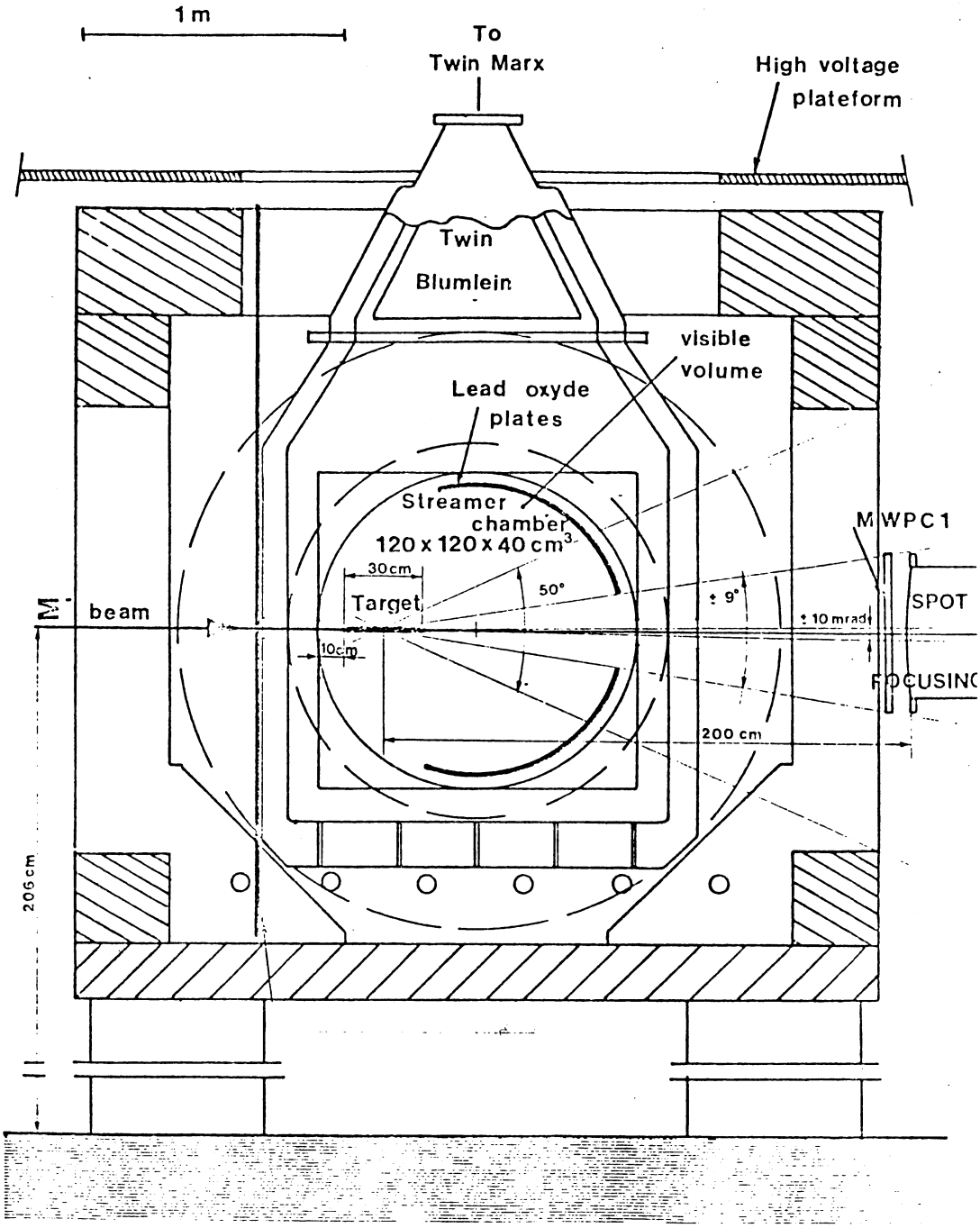

Fig. 5.1 Streamer chamber and magnet

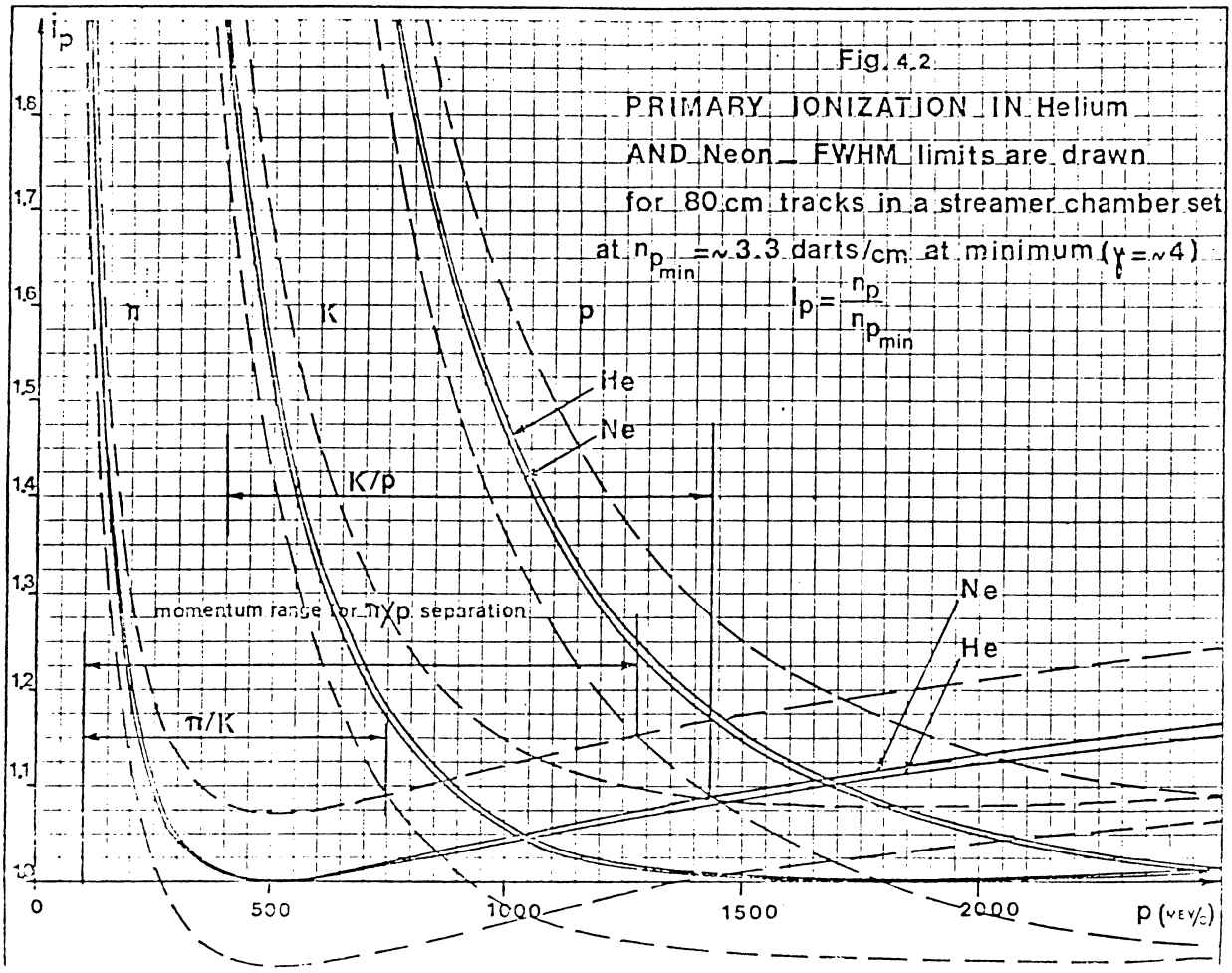

Fig. 5.2 Primary ionization in Helium and Neon FWHM limits are drawn for 80 cm tracks in a streamer chamber set at $n_{p_{min}} = \sim 3.3$ darts/cm at minimum ($\gamma = \sim 4$) $i_p = n_p / n_{p_{min}}$

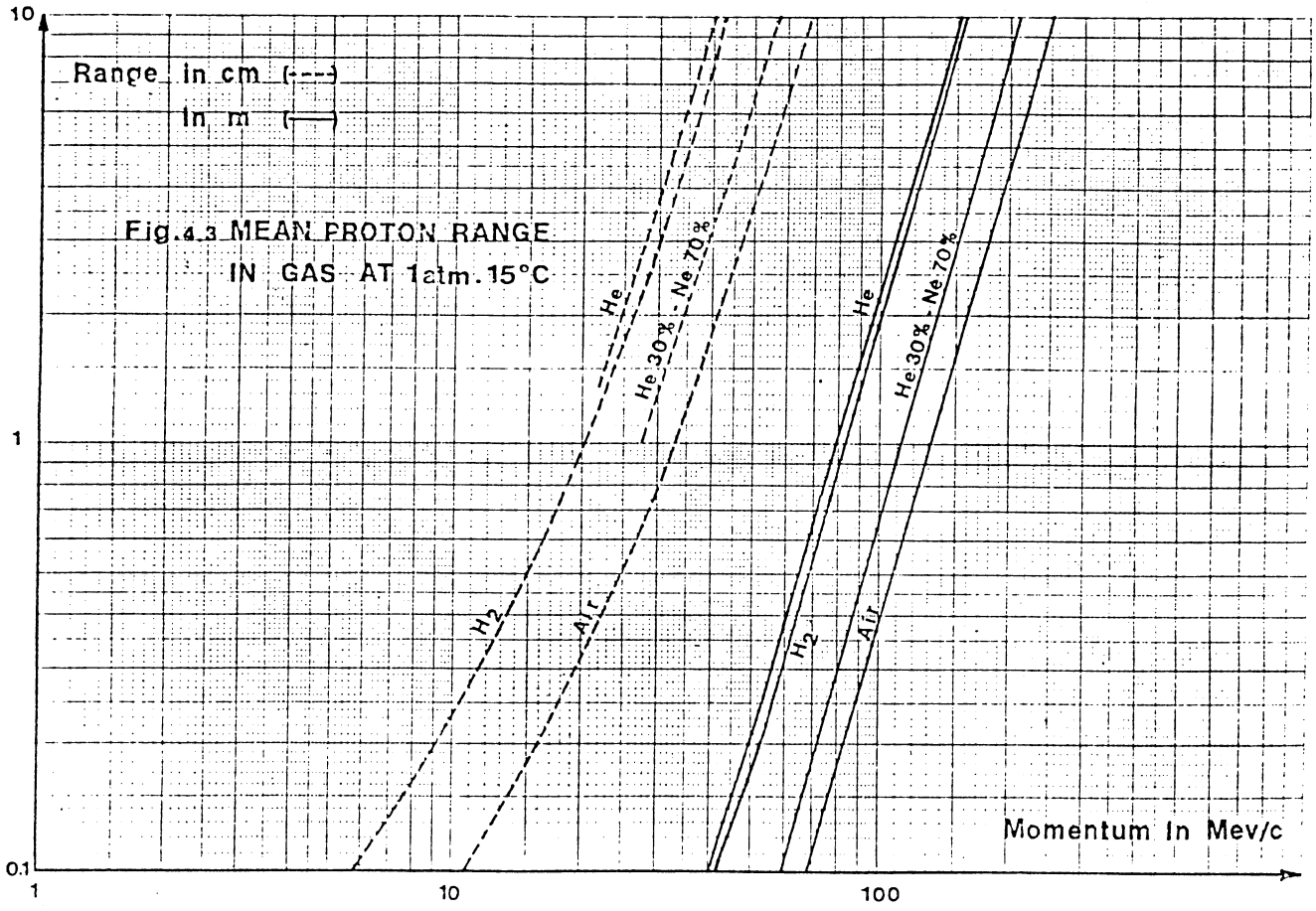

Fig.5.3 Mean proton range in gas at 1 atm.15°C

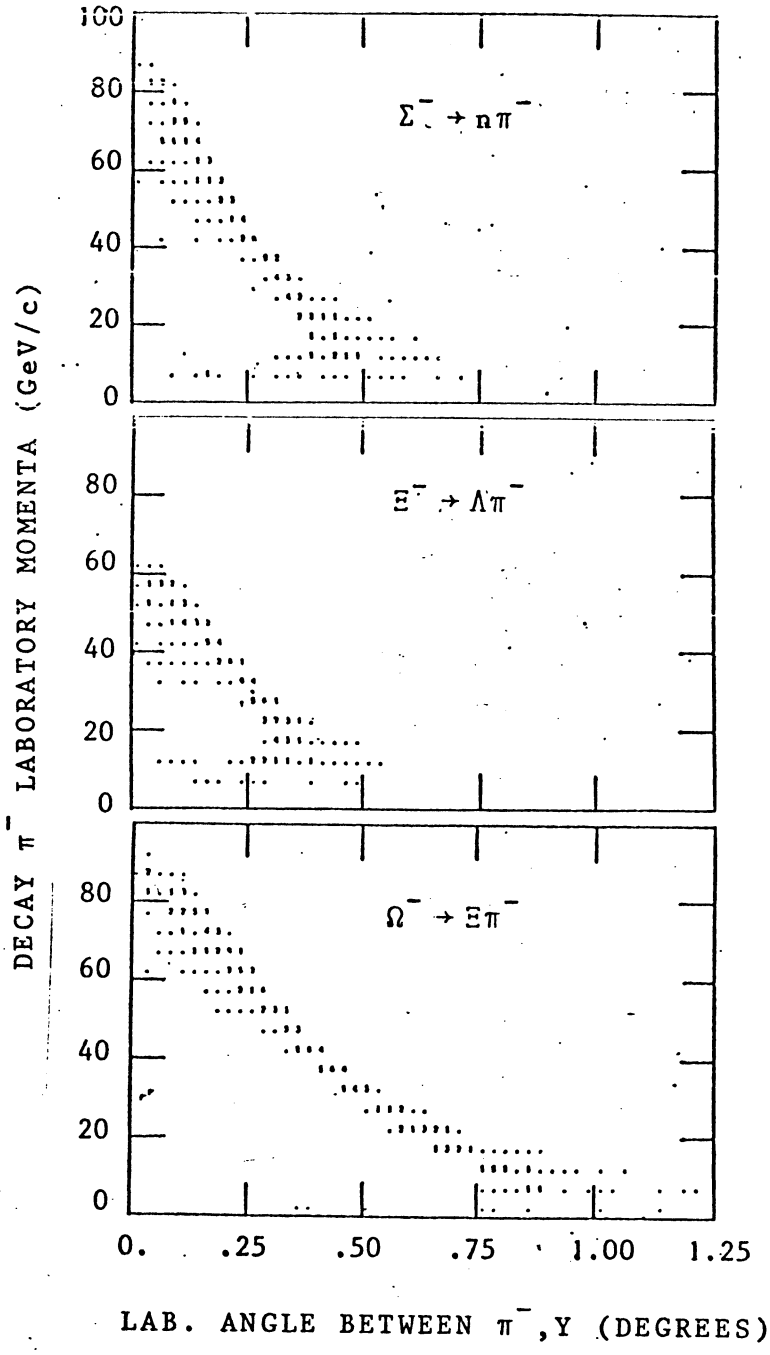

Fig.7.1 Laboratory momentum of the decay π^- versus its decay angle defined in the laboratory system as the angle between the outgoing hyperon and the π^-. The plots were obtained by generating peripheral $Yp \to Yp\pi^+\pi^-\pi^o$ events (see text)